Oxidation of Ruthenium(II) and Ruthenium(III) Porphyrins. Crystal Structures of μ-Oxo-bis[(p-methylphenoxo)(meso-tetraphenylporphyrinato)-ruthenium(IV)] and Ethoxo(meso-tetraphenylporphyrinato)-(ethanol)ruthenium(III)-Bisethanol

J. P. Collman,*[1a] C. E. Barnes,[1a] P. J. Brothers,[1a] T. J. Collins,[1a] T. Ozawa,[1a] J. C. Gallucci,[1b] and James A. Ibers*[1b]

Contribution from the Departments of Chemistry, Stanford University, Stanford, California 94305, and Northwestern University, Evanston, Illinois 60201.
Received October 19, 1983

Abstract: The synthesis of a series of dinuclear Ru(IV) μ-oxo complexes $[Ru(Por)(OR)]_2O$ and $[Ru(Por)X]_2O$ (Por = OEP, TPP, T-*n*-PrP; OR = OCH_3, OC_2H_5, p-$OC_6H_4CH_3$, o-OC_6H_4OH; X = Br, Cl, CF_3CO_2, HSO_4) by *tert*-butyl hydroperoxide oxidation of Ru(Por)(CO)(R'OH) (R' = CH_3, C_2H_5) is described. An X-ray crystal structure determination of $[Ru(TPP)(p\text{-}OC_6H_4CH_3)]_2O$ was carried out. The complex crystallizes in the triclinic space group C_i^1-$P\bar{1}$ with two molecules in a unit cell of dimensions a = 16.911 (11) Å, b = 10.802 (12) Å, c = 12.979 (8) Å, α = 99.96 (3)°, β = 104.31 (2)°, and γ = 77.32 (2)°. Least-squares refinement has led to a final value of the conventional R index (on F^2) of 0.177 based on 7630 independent reflections. The Ru-O(Ru) and Ru-O(p-$OC_6H_4CH_3$) bond lengths are 1.789 (11) and 1.964 (11) Å, respectively, and the Ru-O-Ru angle is 177.8 (7)°. The Ru(IV) μ-oxo complexes can be reduced by $NaBH_4$ or PPh_3 to form the Ru(II) species $Ru(Por)L_2$. $Ru(TPP)(EtOH)_2$ in noncoordinating solvents is oxidized by O_2 to $[Ru(TPP)(OEt)]_2O$, but in the presence of excess ethanol the oxidation halts at a Ru(III) species, Ru(TPP)(OEt)(EtOH)·2EtOH. In noncoordinating solvents this complex is further oxidized by O_2 to the Ru(IV) μ-oxo ethoxide complex. The Ru(III) complex was characterized by an X-ray crystal structure analysis. The complex crystallizes in the triclinic space group C_i^1-$P\bar{1}$ with unit cell parameters a = 9.894 (4) Å, b = 12.946 (6) Å, c = 9.758 (5) Å, α = 112.06 (2)°, β = 94.12 (2)°, γ = 71.85 (2)°, and one molecule per unit cell. Least-squares refinement based on 5073 unique reflections led to a final R index (on F^2) of 0.106. The centrosymmetric complex exhibits one Ru-O bond length of 2.019 (3) Å. These results demonstrate the solvent dependence of the interactions of oxygen with ruthenium porphyrins. The Ru(III) complex reported herein is the first to be structurally characterized.

The importance of heme group chemistry has long been recognized in many areas of the natural sciences. Synthetic iron porphyrin complexes are well established as models for heme systems and continue to yield significant results in the areas of oxygen transport and activation.[2] In contrast, the study of ruthenium porphyrins was begun only a decade ago.[3] Interest in ruthenium porphyrin chemistry has been spurred by possible applications to energy conversion processes based on light-driven reactions and the activation of small molecules (O_2, N_2) of biological interest.[4-7] A better understanding of the unique chemistry of ruthenium porphyrin complexes should yield further understanding of these areas and of high oxidation state intermediates in the cytochrome P450 and horseradish peroxidase catalytic cycles.[2b]

The first ruthenium porphyrin complex was described in 1969,[3] although two years later a corrected formulation of the complex, Ru(TPP)(CO)(EtOH), was published.[7] Currently, all synthetic methods for the insertion of ruthenium into porphyrins yield ruthenium(II) carbonyl products. Structural, spectroscopic, electrochemical, and photoredox studies of these species have been reported over the last decade.[8,9] The chemistry, however, has been restricted primarily to studies of ligand exchange at the sixth coordination site.[10] The difficulty encountered in removing the tenaciously bound carbonyl ligand has had a marked effect on the development of ruthenium porphyrin chemistry. The presence of the carbonyl ligand, a strong π acid, renders the Ru(II) center inactive toward other π acids such as O_2 and N_2. Direct substitution of the CO ligand has been achieved only by employing other strongly coordinating ligands such as NO and PPh_3.[7,11]

Two more general routes for removal of the CO moiety have been developed recently. Photochemical ejection of the carbonyl ligand in a suitable coordinating solvent leads to complexes of the general formula $Ru(Por)(solvent)_2$.[12,13] This route has been exploited in recent years and has led to some fruitful areas of ruthenium porphyrin chemistry. For example, pyrolysis of the $Ru(Por)(py)_2$ complexes prepared by this method yields the novel metal-metal bonded dimers $[Ru(Por)]_2$.[5,14]

(1) (a) Stanford University. (b) Northwestern University.
(2) (a) Collman, J. P. *Acc. Chem. Res.* **1977**, *10*, 265-272. (b) Collman, J. P.; Halbert, T. R.; Suslick, K. S. In "Metal Ion Activation of Dioxygen"; Spiro, T. G., Ed.; Wiley: New York, 1980; Chapter 1. (c) Traylor, T. G. *Acc. Chem. Res.* **1981**, *14*, 102-109.
(3) Fleischer, E. B.; Thorp, R.; Venerable, D. *J. Chem. Soc., Chem. Commun.* **1969**, 475.
(4) (a) Young, R. C.; Nagle, J. K.; Meyer, T. J.; Whitten, D. G. *J. Am. Chem. Soc.* **1978**, *100*, 4773-4778. (b) Hopf, F. R.; Whitten, D. G. *Ibid.* **1976**, *98*, 7422-7424.
(5) Collman, J. P.; Barnes, C. E.; Collins, T. J.; Brothers, P. J.; Gallucci, J.; Ibers, J. A. *J. Am. Chem. Soc.* **1981**, *103*, 7030-7032.
(6) (a) Farrell, N.; Dolphin, D. H.; James, B. R. *J. Am. Chem. Soc.* **1978**, *100*, 324-326. (b) Dolphin, D.; Addison, A. W.; Cairns, M.; Dinello, R. K.; Farrell, N. P.; James, B. R.; Paulson, D. R.; Welborn, C. *Int. J. Quantum Chem.* **1979**, *16*, 311-329. (c) Paulson, D. R.; Addison, A. W.; Dolphin, D.; James, B. R. *J. Biol. Chem.* **1979**, *254*, 7002-7006.
(7) Chow, B. C.; Cohen, I. A. *Bioinorg. Chem.* **1971**, *1*, 57-63.
(8) (a) Little, R. G.; Ibers, J. A. *J. Am. Chem. Soc.* **1973**, *95*, 8583-8590. (b) Bonnet, J. J.; Eaton, S. S.; Eaton, G. R.; Holm, R. H.; Ibers, J. A. *Ibid.* **1973**, *95*, 2141-2149.
(9) (a) Brown, G. M.; Hopf, F. R.; Ferguson, J. A.; Meyer, T. J.; Whitten, D. G. *J. Am. Chem. Soc.* **1973**, *95*, 5939-5942. (b) Rillema, D. P.; Nagle, J. K.; Barringer, L. F., Jr.; Meyer, T. J. *Ibid.* **1981**, *103*, 56-62.
(10) (a) Eaton, S. S.; Eaton, G. R.; Holm, R. H. *J. Organomet. Chem.* **1971**, *32*, C52-C54. (b) Eaton, S. S.; Eaton, G. R.; Holm, R. H. *Ibid.* **1972**, *39*, 179-195. (c) Eaton, S. S.; Eaton, G. R. *Inorg. Chem.* **1977**, *16*, 72-75.
(11) (a) Srivastava, T. S.; Hoffman, L.; Tsutsui, M. *J. Am. Chem. Soc.* **1972**, *94*, 1385-1386. (b) Boschi, T.; Bontempelli, G.; Mazzocchin, G.-A. *Inorg. Chim. Acta* **1979**, *37*, 155-160.
(12) Antipas, A.; Buchler, J. W.; Gouterman, M.; Smith, P. D. *J. Am. Chem. Soc.* **1978**, *100*, 3015-3024.
(13) Abbreviations: Por, porphyrinato dianion unspecified; OEP, 2,3,7,8,12,13,17,18-octaethylporphyrinato dianion; TPP, 5,10,15,20-tetraphenylporphyrinato dianion; T-*n*-PrP, 5,10,15,20-tetra-*n*-propylporphyrinato dianion; bpy, bispyridine; Et, ethyl; Me, methyl; 1-MeIm, 1-methylimidazole; py, pyridine; TBHP, *tert*-butyl hydroperoxide; THF, tetrahydrofuran; trpy, terpyridine.

0002-7863/84/1506-5151$01.50/0

Oxidative methods for removal of the carbonyl ligand were investigated early in the history of ruthenium porphyrin chemistry.[7] It was demonstrated that the presence of the carbonyl ligand rendered the metal center more resistant to electrochemical oxidation.[9,15] Chow and Cohen attempted chemical oxidations[7] but found that, with the exception of air in the presence of cyanide ion, all the oxidizing agents tried either had no effect on Ru(TPP)(CO)(EtOH) or caused complete oxidative decomposition of the porphyrin ring. In contrast, the osmium analogue Os(OEP)(CO)(py) can be oxidized by H_2O_2 to yield $Os^{VI}(OEP)(O)_2$.[16] Recently Masuda et al. described the preparation of $[Ru^{IV}(OEP)(OH)]_2O$ by *tert*-butyl hydroperoxide (TBHP) oxidation of Ru(OEP)(CO)L in benzene solution.[17] Full synthetic details were not reported, but structural and spectroscopic characterization was carried out.

We have also been pursuing this chemistry and report herein the synthesis of a series of complexes $[Ru^{IV}(Por)X]_2O$ where X is an anionic ligand. These species are prepared by two independent routes: (i) TBHP oxidation of Ru(Por)(CO)(EtOH) and (ii) the interaction of dioxygen with ruthenium(II) and -(III) precursors. Several studies of the interaction of molecular oxygen with ruthenium porphyrins have been reported in recent years,[6,4b] but definitive evidence for a ruthenium(II) porphyrin dioxygen complex has not yet been obtained. We have characterized, for the first time, the final products of the reactions of Ru(II) and Ru(III) porphyrins with molecular oxygen. The formation of stable Ru(III) and Ru(IV) porphyrin complexes by this route provides an interesting contrast with the chemistry of the iron porphyrin analogues. The production of Ru(IV) porphyrins by the oxidation of Ru(II) and especially Ru(III) porphyrins with molecular oxygen is striking.

Experimental Section

Ultraviolet and visible spectra were recorded on a Cary Model 219 recording spectrophotometer. Infrared spectra were measured on a Beckman Acculab 3. ^1H NMR spectra were obtained on either a Varian XL-100 instrument or on the Stanford Magnetic Resonance Laboratory Modified Bruker HXS-360 instrument, in both cases employing 5-mm probes and a Nicolet Technology Corporation Model 1180 FT disk data system. Magnetic susceptibility measurements were carried out with a Cahn Faraday Magnetic Susceptibility device. GC analyses were obtained on a HP 5480 gas chromatograph. Elemental analyses and osmometric molecular weight determinations were performed by the Stanford Analytical Laboratory. Field desorption mass spectrometry (FDMS) measurements were carried out at the Middle Atlantic Mass Spectrometry Laboratory at the Johns Hopkins University School of Medicine. Reactions performed under an inert atmosphere were carried out in Schlenkware under nitrogen or argon or in a VAC inert atmosphere chamber under nitrogen.

Materials. Octaethylporphyrin, H_2(OEP), and *meso*-tetraphenylporphyrin, H_2(TPP), were prepared as described in the literature.[18,19] *meso*-Tetra-*n*-propylporphyrin, H_2(T-*n*-PrP), was prepared by a method analogous to that used for H_2(TPP). Ruthenium trichloride and dodecacarbonyltriruthenium(0) were purchased from Alfa. Reagent grade solvents were used without further purification. The preparation and characterization of Ru(TPP)(CO)(py) (**7a**),[8,9a] Ru(OEP)(CO)(py) (**7b**),[12,14] Ru(TPP)(py)$_2$ (**8a**),[7] and Ru(OEP)(py)$_2$ (**8b**)[12,14] have been described previously. Complexes **7a** and **7b** were prepared by recrystallization of Ru(TPP)(CO)(EtOH) (**1a**) and Ru(OEP)(CO)(MeOH) (**2a**), respectively, in the presence of pyridine. The procedure described by Antipas et al.[12] was used to prepare compounds **8a** and **8b**. The preparation of [Ru(TPP)]$_2$ (**9a**) and [Ru(OEP)]$_2$ (**9b**) is described in ref 5. Deuterated solvents for NMR studies were dried over molecular sieves. Purified reagent grade solvents or spectroscopic grade solvents were used for the quantitative measurement of electronic absorption spectra.

Syntheses. (*meso*-Tetraphenylporphyrinato)carbonyl(ethanol)ruthenium(II) [Ru(TPP)(CO)(EtOH) (1a)]. Ruthenium trichloride (1.0 g) was suspended in ethyl digol [2-(2′-methoxyethoxy)ethanol] (20 mL) under CO, and the suspension was heated to 150 °C until the solution was pale yellow. The solution was cooled and then added dropwise under N_2 over the course of 1 h to a suspension of H_2(TPP) (1.5 g) in ethyl digol (30 mL) at 150 °C. The reaction was monitored by visible spectroscopy and heating was discontinued when the characteristic spectrum of H_2(TPP) was no longer evident (usually ca. 90 min). A solution of NaCl in water was added to the cooled, filtered solution. The mixture was stirred for 2 h to aid flocculation of the precipitate and then filtered through a Celite pad, washed with water, and dried under vacuum. The product was washed off the Celite pad with a solution of 5% EtOH in CH_2Cl_2 and chromatographed on silica gel. The same solvents were used to elute the bright orange leading band that contained the product. After addition of more ethanol to the eluate the solvent volume was reduced and crystals of the dark orange-red product precipitated. This product was contaminated by an impurity, presumed to be a chlorin, that exhibited a band at ca. 600 nm in the visible spectrum. Oxidation of the product by DDQ (2,3-dichloro-5,6-dicyano-1,4-benzoquinone) by the method of Rousseau and Dolphin[18b] yielded pure Ru(TPP)(CO)(EtOH) (1.1 g, 57%).

Anal. Calcd for $C_{47}H_{34}N_4O_2Ru$: C, 71.65; H, 4.35; N, 7.11. Found: C, 71.43; H, 4.40; N, 7.15.

NMR ($CDCl_3$, 100 MHz): H_β 8.68 (s); H_o 8.16 (m); H_m, H_p 7.69 (m); CH_3 −0.05 (t); CH_2 −1.65 (b s); OH 0.75 (b s) ppm. UV/vis (CH_2Cl_2): λ_{max} 412 (Soret), 532 nm. IR (Nujol): ν_{CO} 1948 cm^{-1}.

(*meso*-Tetra-*n*-propylporphyrinato)carbonyl(ethanol)ruthenium(II) [Ru(T-*n*-PrP)(CO)(EtOH) (1b)]. To a solution of dodecacarbonyltriruthenium(0) (112 mg) in toluene under nitrogen was added H_2(T-*n*-PrP) (100 mg), and the reaction mixture was heated under reflux for 24 h. The solvent was removed under reduced pressure and the product purified by column chromatography (SiO_2, 60–200 mesh, 1 g, CH_2Cl_2–EtOH, 49:1). A wine-red band was collected and passed down a similar column with the use of toluene as the eluant. The product was recrystallized from dichloromethane–hexane or dichloromethane–ethanol–water to yield violet-black crystals that were collected and dried at 140 °C in vacuo (57.6 mg, 50%).

Anal. Calcd for $C_{35}H_{42}N_4O_2Ru$: C, 64.49; H, 6.50; N, 8.60. Found: C, 64.49; H, 6.34; N, 8.87.

NMR ($CDCl_3$, 100 MHz): H_β 9.35 (s); $CH_2CH_2CH_3$ 4.82 (8.3 Hz, t); $CH_2CH_2CH_3$ 2.35 (7.9 Hz, m); $CH_2CH_2CH_3$ 1.31 (7.5 Hz, t); $HOCH_2CH_3$ 0.20 (m); $HOCH_2CH_3$ −0.57 (7.5 Hz, t); OH −2.54 (s) ppm. UV/vis (1.9×10^{-5} M, CH_2Cl_2): λ_{max} (log ϵ) 411 (5.17), 533 (4.07), 567 (3.54) nm.

(Octaethylporphyrinato)carbonyl(methanol)ruthenium(II) [Ru(OEP)(CO)(MeOH) (1c)]. H_2(OEP) (1 g, 1.8 mmol) was dissolved in ethyl digol (500 mL) and heated to refluxing temperature under a carbon monoxide atmosphere. $RuCl_3 \cdot H_2O$ (940 mg, 2 equiv) was dissolved in ethyl digol (50 mL) and added dropwise to the boiling solution over the course of 3 h and then heated under reflux for an additional 2 h. The extent of reaction was measured by TLC (SiO_2; CH_2Cl_2) or UV/vis spectra of aliquots of the reaction mixture. When no H_2(OEP) was detected by TLC or UV/vis methods, the solution was cooled and flushed with argon. The volume was reduced to 50 mL on a rotary evaporator, and distilled water (100 mL) was added quickly to precipitate all porphyrinic material. The solution was filtered through Celite and the precipitate washed with water, dried, and redissolved in CH_2Cl_2. Silica gel (100 cm^3) was added to the solution which was then vigorously stirred. Filtration yielded a translucent bright-red solution for which TLC showed one pink spot (R_f 0.98) with no origin material. The solution volume was reduced to 200 mL and then methanol (40 mL) and water (10 drops) were added. The solution volume was further reduced to 50 mL and refrigerated overnight. The resulting crystals of the product were filtered, washed with methanol, and dried under vacuum (780 mg, 60%).

Anal. Calcd for $C_{38}H_{48}N_4O_2Ru$: C, 65.77; H, 6.97; N, 8.07. Found: C, 65.53; H, 7.02; N, 8.13.

NMR ($CDCl_3$, 100 MHz): H_{meso} 9.95 (s); CH_2CH_3 4.11 (7.6 Hz, q); CH_2CH_3 1.94 (7.6 Hz, q); OCH_3 −2.3 (s); $HOCH_3$ ~−0.5 (b s) ppm. UV/vis (C_6H_6): λ_{max} (log ϵ) 393 (5.16), 517 (4.06), 549 (4.38) nm. IR (KBr): ν_{CO} 1945, 1928 cm^{-1}.

μ-Oxo-bis[methoxo(*meso*-tetraphenylporphyrinato)ruthenium(IV)] [[Ru(TPP)(OMe)]$_2$O (2a)]. Ru(TPP)(CO)(EtOH) (**1a**) (1 g) was suspended in benzene–ethanol (100 mL, 1:1), and *tert*-butyl hydroperoxide (10 mL) was added. When the starting material was totally consumed

(14) (a) Sovocool, G. W.; Hopf, F. R.; Whitten, D. G. *J. Am. Chem. Soc.* **1972**, *94*, 4350–4351. (b) Hopf, F. R.; O'Brien, T. P.; Scheidt, W. R.; Whitten, D. G. *J. Am. Chem. Soc.* **1975**, *97*, 277–281.
(15) Brown, G. M.; Hopf, F. R.; Meyer, T. J.; Whitten, D. G. *J. Am. Chem. Soc.* **1975**, *97*, 5385–5390.
(16) Buchler, J. W.; Smith, P. D. *Angew. Chem., Int. Ed. Engl.* **1974**, *13*, 341.
(17) Masuda, H.; Taga, T.; Osaki, K.; Sugimoto, H.; Mori, M.; Ogoshi, H. *J. Am. Chem. Soc.* **1981**, *103*, 2199–2203.
(18) (a) Smith, K. M., Ed. "Porphyrins and Metalloporphyrins"; Elsevier: Amsterdam, 1975. (b) Rousseau, K.; Dolphin, D. *Tetrahedron Lett.* **1974**, 4251–4254.
(19) (a) Engelsma, G.; Yamamoto, A.; Markham, E.; Calvin, M. *J. Phys. Chem.* **1962**, *66*, 2517–2531. (b) Whitlock, H. W.; Hanauer, R. *J. Org. Chem.* **1968**, *33*, 2169–2171.

in the reaction, as determined by TLC (SiO_2; CH_2Cl_2–EtOH, 19:1), a solution of sodium cyanate (5 g) in water (100 mL) was added. The benzene was removed at room temperature on a rotary evaporator. The solid material was collected, washed with water, dried, and purified by column chromatography (SiO_2, 60–200 mesh, 200 g; CH_2Cl_2–EtOH, 19:1). Recrystallization from dichloromethane–methanol yielded violet-black crystals that were dried at 140 °C in vacuo (920 mg, 96%).

Anal. Calcd for $C_{90}H_{62}N_8O_3Ru_2$: C, 71.79; H, 4.15; N, 7.44. Found: C, 71.44; H, 4.23; N, 7.39.

NMR ($CDCl_3$–MeOH, 100 MHz): H_β 8.54 (s); H_o 8.90 (m), 7.34 (m); H_m, H_p 7.94 (m), 7.79 (m), 7.52 (m) (J_{phenyl} = 7.4 Hz); OCH_3 −3.99 (s) ppm. UV/vis (5×10^{-5} M, CH_2Cl_2): λ_{max} (log ϵ) 398 (5.26), 529 (4.42) sh, 549 (4.51), 584 (4.24) sh nm.

μ-Oxo-bis[ethoxo(*meso*-tetraphenylporphyrinato)ruthenium(IV)] [[Ru(TPP)(OEt)]$_2$O·2H$_2$O (2b)]. Recrystallization of [Ru(TPP)(OMe)]$_2$O (**2a**) from dichloromethane–ethanol yielded violet-black crystals. The ^{1}H NMR spectra ($CDCl_3$, CD_2Cl_2) demonstrated that this compound often contained mixed ethoxide and hydroxide ligation, with trace amounts of water in the solvent giving rise to the hydroxide ligands. In the presence of excess ethanol a full complement of coordinated ethoxide signals is observed.

Anal. Calcd for $C_{92}H_{70}N_8O_5Ru$: C, 70.39; H, 4.49; N, 7.14. Found: C, 70.30; H, 4.13; N, 7.18.

NMR ($CDCl_3$–EtOH, 360 MHz): H_β 8.52 (s); H_o 8.92 (d), 7.34 (d); H_m, H_p 7.94 (t), 7.79 (t), 7.51 (t) (J_{phenyl} = 7.4 Hz); OCH_2CH_3 −3.86 (6.5 Hz, t); OCH_2CH_3 −4.03 (6.5 Hz, q) ppm. UV/vis (5×10^{-5} M, CH_2Cl_2–EtOH 1:1): λ_{max} (log ϵ) 398 (5.26), 530 (4.40) sh, 552 (4.50), 589 (4.18) sh nm.

μ-Oxo-bis[(*p*-methylphenoxo)(*meso*-tetraphenylporphyrinato)ruthenium(IV)] [[Ru(TPP)(*p*-OC$_6$H$_4$CH$_3$)]$_2$O (2c)]. [Ru(TPP)(OEt)]$_2$O (**2b**) (30 mg) was dissolved in dichloromethane (5 mL), and ethanol (20 mL) containing *p*-cresol (200 mg) was added. The solution was heated under reflux (10 min) and allowed to stand at room temperature. The violet-black crystals were collected, washed with ethanol, and dried in vacuo at 140 °C (31 mg, 96%).

Anal. Calcd for $C_{102}H_{70}N_8O_3Ru_2$: C, 73.90; H, 4.26; N, 6.76. Found: C, 73.55; H, 4.48; N, 6.74.

NMR ($CDCl_3$–*p*-$HOC_6H_4CH_3$, 360 MHz): H_β 8.57 (s); H_o 8.93 (d), 7.21 (d); H_m, H_p 7.98 (t), 7.83 (t), 7.55 (t) (J_{phenyl} = 7.5 Hz); CH_3 1.23 (s); *p*-$OC_6H_4CH_3$ 4.68 (9.0 Hz, d), −0.15 (9.0 Hz, d) ppm. UV/vis (5×10^{-5} M, 0.1 M *p*-$HOC_6H_4CH_3$ in CH_2Cl_2): λ_{max} (log ϵ) 391 (5.32), 530 (4.31) sh, 553 (4.42), 563 (4.41) sh, 587 (4.29) sh nm.

μ-Oxo-bis[(*o*-hydroxyphenoxo)(*meso*-tetraphenylporphyrinato)ruthenium(IV)] [[Ru(TPP)(*o*-OC$_6$H$_4$OH)]$_2$O (2d)]. This compound was produced in a manner similar to the preparation of [Ru(TPP)(*p*-$OC_6H_4CH_3$)]$_2$O (**2c**) (32 mg, 98%).

Anal. Calcd for $C_{100}H_{66}N_8O_5Ru_2$: C, 72.27; H, 4.00; N, 6.74. Found: C, 71.90; H, 4.13; N, 6.74.

NMR (CD_2Cl_2, 100 MHz): H_β 8.68 (s); H_o 9.00 (m), 7.27 (m); H_m, H_p 8.04 (m), 7.88 (m), 7.60 (m) (J_{phenyl} = 7.5 Hz); *o*-C_6H_4OH 5.08 (7.5 Hz, m); −0.45 (7.5 Hz, m); OH −2.50 (s) ppm. UV/vis (5×10^{-5} M, 0.1 M *o*-HOC_6H_4OH in CH_2Cl_2): λ_{max} (log ϵ) 392 (5.38), 532 (4.22) sh, 554 (4.32), 564 (4.31) sh, 587 (4.24) sh nm.

μ-Oxo-bis[chloro(*meso*-tetraphenylporphyrinato)ruthenium(IV)] [[Ru(TPP)Cl]$_2$O (2e)]. [Ru(TPP)(OEt)]$_2$O (**2b**) (30 mg) was dissolved in dichloromethane (5 mL), and ethanol (15 mL) and concentrated HCl (2 mL) were added. The solution was heated under reflux (10 min). As the solvent volume was reduced, red-violet crystals of the product formed. These were collected, washed with ethanol, and dried at 140 °C under vacuum (29 mg, 98%).

Anal. Calcd for $C_{88}H_{56}Cl_2N_8ORu_2$: C, 69.79; H, 3.73; N, 7.40; Cl, 4.68. Found: C, 69.54; H, 3.83; N, 7.28; Cl, 4.27.

UV/vis(5×10^{-5} M, CH_2Cl_2–CH_3CH_2OH–HCl 1:1:0.04): λ_{max} (log ϵ) 394 (5.45), 494 (3.92) sh, 534 (4.01) sh, 554 (4.09), 604 (4.01) sh, 630 (4.06) nm. NMR: not obtained as compound is not sufficiently soluble.

μ-Oxo-bis[bromo(*meso*-tetraphenylporphyrinato)ruthenium(IV)] [[Ru(TPP)Br]$_2$O (2f)]. This compound was produced by the reaction of [Ru(TPP)(OEt)]$_2$O (**2b**) with HBr, as in the preparation of [Ru(TPP)Cl]$_2$O (**2e**) (29 mg, 92%).

Anal. Calcd for $C_{88}H_{56}Br_2N_8ORu_2$: C, 65.92; H, 3.52; N, 6.99. Found: C, 66.30; H, 3.79; N, 6.96.

NMR, UV/vis: not recorded as compound is not sufficiently soluble.

μ-Oxo-bis[(*meso*-tetraphenylporphyrinato)(trifluoroacetato)ruthenium(IV)] [[Ru(TPP)(O$_2$CCF$_3$)]$_2$O (2g)]. [Ru(TPP)(OEt)]$_2$O (**2b**) (30 mg) was dissolved in dichloromethane (5 mL). Ethanol (15 mL) containing concentrated CF_3CO_2H (2 mL) was added. The solvent volume was lowered under reduced pressure to ca. 8 mL, and the solution was allowed to stand for several days in an ethanol-saturated atmosphere. The violet-black crystals were collected, washed with ethanol–water (1:1), and dried at 140 °C under vacuum (31 mg, 95%).

Anal. Calcd for $C_{92}H_{56}F_6N_8O_5Ru_2$: C, 66.18; H, 3.38; N, 6.71. Found: C, 66.62; H, 3.56; N, 6.61.

Molecular weight (osmometric, C_6H_6): calcd 1670; found 1730. Mass spectrum (field desorption): moderate signals in the 1660–1676 m/z range correspond closely to the theoretical distribution for the molecular ion species; weak signals (1554–1564 m/z and 1438–1447 m/z) correspond to losses of one and both $CF_3CO_2^-$ ligands. NMR ($CDCl_3$, 360 MHz): H_β 8.74 (s); H_o 8.93 (d), 7.29 (d); H_m, H_p 8.03 (t); 7.87 (t); 7.56 (t) (J_{phenyl} = 7.5 Hz) ppm. UV/vis (5×10^{-5} M, CH_2Cl_2–CH_3CH_2OH–CF_3CO_2H 2.5:1:0.3): λ_{max} (log ϵ) 389 (5.49), 530 (4.07) sh, 549 (4.12), 599 (3.96) sh, 640 (4.10) nm.

μ-Oxo-bis[bisulfato(*meso*-tetraphenylporphyrinato)ruthenium(IV)] [[Ru(TPP)(OSO$_3$H)]$_2$O (2h)]. This compound was prepared by the reaction of [Ru(TPP)(OEt)]$_2$O (**2b**) with H_2SO_4, as in the preparation of [Ru(TPP)(O$_2$CCF$_3$)]$_2$O (**2g**) (24 mg, 75%).

Anal. Calcd for $C_{88}H_{58}N_8O_9Ru_2S_2$: C, 64.54; H, 3.57; N, 6.84. Found: C, 64.47; H, 3.79; N, 6.62.

μ-Oxo-bis[methoxo(octaethylporphyrinato)ruthenium(IV)] [[Ru(OEP)(OMe)]$_2$O (3a)]. Ru(OEP)(CO)(MeOH) (**1c**) (100 mg) was ground to a fine powder and then dissolved in benzene (100 mL) and 2-propanol (100 mL). *tert*-Butyl hydroperoxide (130 mg) in benzene (5 mL) was added to the stirred solution. When the starting material was totally consumed (TLC, SiO_2; CH_2Cl_2) the solvent volume was lowered to 100 mL under reduced pressure. 2-Propanol (50 mL) was added and the solvent volume reduced under the same conditions to 50 mL. Methanol (50 mL) and water sufficient to effect complete precipitation of the porphyrin were added. The solid was collected on a Celite pad, washed with water, and dissolved in methanol. The solvent was removed under reduced pressure and the product purified by column chromatography (SiO_2, 60–200 mesh, 1 g; toluene–methanol, 99:1, to remove trace quantities of starting material, then toluene–methanol, 9:1). The product was recrystallized from a carefully layered solution of porphyrin in methanol over methanol–water (9:1) saturated with sodium cyanate to effect salting out (95 mg, 98%). The crystals were collected, washed with water, and dried at 140 °C in vacuo.

Molecular weight (osmometric, C_6H_6): calcd from $C_{74}H_{94}N_8O_3Ru_2$ 1346; found 1350. NMR (C_6D_6, 360 MHz): H_{meso} 9.40 (s); CH_2CH_3 4.37 (m), 3.99 (m); CH_2CH_3 2.86 (t); OCH_3 −3.45 (s) ppm. UV/vis (0.3 $\times 10^{-5}$ M, 0.1 M MeOH in CH_2Cl_2): λ_{max} (log ϵ) 376 (5.29), 511 (3.10), 580 (4.38) nm.

μ-Oxo-bis[chloro(octaethylporphyrinato)ruthenium(IV)] [[Ru(OEP)Cl]$_2$O (3b)]. [Ru(OEP)(OMe)]$_2$O (**3a**) (20 mg) was suspended in methanol (20 mL) and vigorously stirred as concentrated hydrochloric acid (0.5 mL) was added dropwise. All the solid material dissolved and the dark-green solution turned red. Water (0.5 mL) was added dropwise to the stirred solution, and the solvent volume was lowered under reduced pressure until the first crystals were visible. The solution was allowed to stand until crystallization was complete and the mother liquor had become colorless. The microcrystalline material was collected on a Celite pad, washed with water, and dried in vacuo at 25 °C. The solid was washed through the Celite pad with dichloromethane, and the solution was filtered again through a fine porosity sintered glass crucible. Crystallization to afford dark crystals was effected by vapor diffusion of cyclohexane into a dichloromethane solution of the product (2 mL). The solid product was dried at 140 °C in vacuo (19.1 mg, 95%).

Anal. Calcd for $C_{72}H_{88}Cl_2N_8ORu_2$: C, 63.84; H, 6.54; N, 8.27. Found: C, 64.19; H, 6.42; N, 8.12.

NMR (C_6D_6, 360 MHz): H_{meso} 9.42 (s); CH_2CH_3 4.31 (m), 4.00 (m); CH_2CH_3 1.92 (t) ppm. UV/vis ($CHCl_3$): λ_{max} 383 (Soret), 494, 554, 604, 684 nm.

μ-Oxo-bis[hydroxo(octaethylporphyrinato)ruthenium(IV)] [[Ru(OEP)(OH)]$_2$O (3c)]. The preparation of this complex is described in ref 5.

NMR (C_6D_6, 360 MHz): H_{meso} 9.40 (s); CH_2CH_3 4.40 (m), 4.05 (m); CH_2CH_3 1.90 (t); OH −9.40 (s) ppm. UV/vis (C_6H_6): λ_{max} 375 (Soret), 512, 561 nm.

μ-Oxo-bis[methoxo(*meso*-tetra-*n*-propylporphyrinato)ruthenium(IV)] [[Ru(T-*n*-PrP)(OMe)]$_2$O (4a)]. Ru(T-*n*-PrP)(CO)(EtOH) (**1b**) (50 mg) was dissolved in benzene (100 mL) and 2-propanol (100 mL). *tert*-Butyl hydroperoxide (3 mL) was added to the stirred solution. When the starting material was totally consumed in the reaction, as determined by TLC (SiO_2; CH_2Cl_2–EtOH, 19:1), the solvent volume was lowered to 50 mL under reduced pressure at 25 °C. 2-Propanol (25 mL) was added and the solvent volume reduced under the same conditions to 25 mL. Methanol (25 mL) and water sufficient to effect complete precipitation of the product were added. The solid material was collected on a Celite pad, washed with water, and dried in vacuo at 25 °C. The solid was washed through the Celite pad with methanol, the solvent was removed under reduced pressure, and the product was purified by column chro-

matography (SiO_2, 60–200 mesh, 1 g; CH_2Cl_2–EtOH, 19:1). The product was crystallized by vapor diffusion of hexane into a dichloromethane–methanol solution. The violet-black crystals were collected, washed with hexane, and dried at 100 °C in vacuo (43.6 mg, 91.5%).

Anal. Calcd for $C_{66}H_{78}N_8O_3Ru_2$: C, 64.26; H, 6.37; N, 9.08. Found: C, 64.36; H, 6.24; N, 8.73.

NMR ($CDCl_3$, 100 MHz): H_β 9.07 (s); $CH_2CH_2CH_3$ 4.70 (7.8 Hz, t); $CH_2CH_2CH_3$ 2.32 (7.7 Hz, m); $CH_2CH_2CH_3$ 1.35 (7.6 Hz, t); OCH_3 −3.58 (s) ppm. UV/vis (3.3×10^{-5} M, CH_2Cl_2): λ_{max} (log ϵ) 394 (4.94), 538 (4.05), 576 (4.00) nm.

μ-Oxo-bis[chloro(*meso*-tetra-*n*-propylporphyrinato)ruthenium(IV)] [[Ru(T-*n*-PrP)Cl]$_2$O (4b)]. [Ru(T-*n*-PrP)(OMe)]$_2$O (**4a**) (8 mg) was dissolved in methanol (10 mL) and the solution was vigorously stirred as concentrated hydrochloric acid (0.5 mL) was added dropwise. On addition of the acid, the wine-red solution changed to a dark green. Water (2 mL) was added dropwise to the stirred solution, and the solvent volume was lowered under reduced pressure until the first crystals were visible. The solution was allowed to stand until crystallization was complete and the mother liquor had become colorless. The solid product was collected, washed with water, and dried at 140 °C in vacuo (7 mg, 87%).

Anal. Calcd for $C_{64}H_{72}Cl_2N_8ORu_2$: C, 61.87; H, 5.84; N, 9.02. Found: C, 60.60; H, 5.64; N, 8.45.

NMR (C_6D_6, 100 MHz): H_β 9.10 (s); $CH_2CH_2CH_3$ 4.88 (8.0 Hz, t); $CH_2CH_2CH_3$ 2.26 (7.6 Hz, m); $CH_2CH_2CH_3$ 1.19 (7.6 Hz, t) ppm.

μ-Oxo-bis[(*meso*-tetra-*n*-propylporphyrinato)(trifluoroacetato)ruthenium(IV)] [[Ru(T-*n*-PrP)(O$_2$CCF$_3$)]$_2$O·H$_2$O (4c)]. [Ru(T-*n*-PrP)(OMe)]$_2$O (**4c**) (8 mg) was dissolved in dichloromethane (2 mL), and ethanol (10 mL) containing trifluoroacetic acid (1 mL) was added. The solvent volume was lowered under reduced pressure to ca. 2 mL, and the solution was allowed to stand for several days under a hexane-saturated atmosphere. The violet-black crystals were collected, washed with hexane, and dried at 140 °C in vacuo (6.0 mg, 66%).

Anal. Calcd for $C_{68}H_{74}F_6N_8O_6Ru_2$: C, 57.70; H, 5.27; N, 7.92. Found: C, 57.75; H, 5.68; N, 7.50.

UV/vis (3.6×10^{-5} M, CH_2Cl_2): λ_{max} (log ϵ) 388 (4.84), 536 (3.42), 580 (3.55), 615 (3.53) nm.

(*meso*-Tetraphenylporphyrinato)bis(tetrahydrofuran)ruthenium(II) [Ru(TPP)(THF)$_2$ (5)]. (a) [Ru(TPP)]$_2$ (**9a**) (10 mg) was dissolved in THF (5 mL) under an inert atmosphere. The solution was degassed, and the evacuated vessel was left to stand for 4 days. Removal of the solvent afforded fine brown crystals of the product in quantitative yield.

(b) [Ru(TPP)(OEt)]$_2$O (**2b**) (10 mg) and $NaBH_4$ (10 mg) were stirred in THF (5 mL) under an inert atmosphere for 30 min. The solution was passed down an alumina column (Activity 1, neutral, 1 × 5 cm) with THF as the eluent. Reduction of the solvent volume yielded the product which was dried in vacuo (9 mg, 88%).

The compound was characterized on the basis of the similarity of the spectral data with other known complexes of the type Ru(Por)L$_2$.[7,12,14]

UV/vis (THF): 405 (Soret), 503 nm. NMR (C_6D_6, 100 MHz): H_β 8.2 (s); H_o 8.1 (m); H_m, H_p 7.7 (m); H_β (THF) 0.3 (br s); H_α (THF) −2.3 (br s) ppm.

(*meso*-Tetraphenylporphyrinato)bis(triphenylphosphine)ruthenium(II) [Ru(TPP)(PPh$_3$)$_2$ (6a)]. (a) [Ru(TPP)(OEt)]$_2$O (**2b**) (30 mg) and triphenylphosphine (100 mg) were dissolved in tetrahydrofuran (5 mL) under an inert atmosphere. A filtered solution of sodium borohydride (50 mg) in ethanol (20 mL) was added, and the reaction mixture was stirred for 2 h. The crystalline product was collected, washed with ethanol, and recrystallized from dichloromethane–ethanol (containing triphenylphosphine) under an inert atmosphere to give violet crystals. These were collected, washed with ethanol, and dried at 140 °C (45 mg, 93%).

(b) This same material was produced by stirring a tetrahydrofuran–ethanol solution of [Ru(TPP)(OCH$_2$CH$_3$)]$_2$O and triphenylphosphine for 20 h or by heating under reflux these two materials in benzene under an inert atmosphere until the reaction was judged complete by UV/vis spectroscopy.

Anal. Calcd for $C_{80}H_{58}N_4P_2Ru$: C, 77.59; H, 4.72; N, 4.53; P, 5.00. Found: C, 77.45; H, 4.88; N, 4.42; P, 5.30.

NMR ($CDCl_3$, 100 MHz): H_β 8.34 (s); H_o (TPP) 7.73 (m); H_m, H_p (TPP) 7.46 (m); H_m, H_p (PPh_3) 6.48 (m); H_o (PPh_3) 4.57 (d) ppm. UV/vis (6.6×10^{-5} M, 0.1 M PPh_3 in CH_2Cl_2): λ_{max} (log ϵ) 412 (4.49), 432 (5.35), 520 (3.99), 548 (3.80) sh nm.

(*meso*-Tetra-*n*-propylporphyrinato)bis(triphenylphosphine)ruthenium(II) [Ru(T-*n*-PrP)(PPh$_3$)$_2$ (6b)]. (a) [Ru(T-*n*-PrP)(OMe)]$_2$O (**4a**) (10 mg) and triphenylphosphine (30 mg) were dissolved in tetrahydrofuran (2 mL) under an inert atmosphere. A filtered solution of sodium borohydride (15 mg) in ethanol (10 mL) was added, and the reaction mixture was stirred for 5 h. The crystalline product was collected, washed with ethanol, and recrystallized from dichloromethane–ethanol under an inert atmosphere to give violet crystals. These were collected, washed with ethanol, and dried at 25 °C in vacuo (15 mg, 84%).

(b) This same material was produced by stirring a tetrahydrofuran–ethanol solution of [Ru(T-*n*-PrP)(OMe)]$_2$O and triphenylphosphine for 24 h under an inert atmosphere.

Anal. Calcd for $C_{68}H_{51}N_4P_2Ru$: C, 74.09; H, 6.04; N, 5.08, P, 5.62. Found: C, 74.03; H, 5.88; N, 5.04; P, 5.48.

UV/vis (2×10^{-5} M, CH_2Cl_2): λ_{max} (log ϵ) 414 (5.01), 433 (5.40), 506 (3.98) nm.

(*meso*-Tetra-*n*-propylporphyrinato)bis(pyridine)ruthenium(II) [Ru(T-*n*-PrP)(py)$_2$ (8c)]. Ru(T-*n*-PrP)(CO)(EtOH) (**1b**) (10 mg) was dissolved in dry pyridine (30 mL) in a quartz cell. The solution was photolyzed under argon with a Hanovia ultraviolet quartz lamp (140 W). The reaction was monitored by visible spectroscopy, and photolysis was discontinued when the characteristic spectrum of the starting material was no longer evident (usually <120 min). The solvent volume was lowered under reduced pressure until crystal formation began. The solution was allowed to stand until crystallization was complete. The purple crystals were collected, washed with cold methanol, and dried in vacuo at 140 °C (7.5 mg, 60%).

Anal. Calcd for $C_{42}H_{46}N_6Ru$: C, 68.55; H, 6.30; N, 11.40. Found: C, 68.03; H, 6.24; N, 11.10.

NMR (C_6D_6, 360 MHz): H_β 9.15 (s); $CH_2CH_2CH_3$ 4.33 (t); $CH_2CH_2CH_3$ 2.57 (m); $CH_2CH_2CH_3$ 1.19 (t) (J_{propyl} = 7.5 Hz); H_p (py) 4.94 (t); H_m (py) 4.35 (t); H_o (py) 2.72 (d) ppm.

Ethoxo(*meso*-tetraphenylporphyrinato)(ethanol)ruthenium(III) [Ru(TPP)(OEt)(EtOH) (10)]. Ru(TPP)(THF)$_2$ (**5**) (20 mg) was dissolved in dichloromethane (10 mL) and ethanol (5 mL) under a nitrogen atmosphere. The solution was exposed to air and the solvent volume reduced on a rotary evaporator. Dark purple crystals of the product formed. These were collected, washed with cold ethanol, and dried (17 mg, 85%).

UV/vis (5% EtOH in CH_2Cl_2): 409 (Soret), 518 nm.

X-ray Data Collection and Structure Solution for [Ru(TPP)(*p*-OC$_6$H$_4$CH$_3$)]$_2$O (2c). Suitable crystals of [Ru(TPP)(*p*-OC$_6$H$_4$CH$_3$)]$_2$O (**2c**) were obtained from a solution of dichloromethane and ethanol. Preliminary precession photographs taken with Cu Kα radiation revealed only the required inversion center, consistent with $P1$ or $P\bar{1}$ as the space group. The crystal used for data collection was a violet-black rectangular-shaped rod. At −157 °C the lattice parameters are a = 16.911 (11) Å, b = 19.802 (12) Å, c = 12.979 (8) Å, α = 99.96 (3)°, β = 104.31 (2)°, and γ = 77.53 (2)°. These were determined by the least-squares analysis of the setting angles for 20 reflections in the range $20 < 2\theta < 29°$ (Mo Kα_1) that had been centered on a Picker FACS-I diffractometer.

Crystallographic details for this compound may be found in Table I. Intensity data were collected by standard techniques.[20,21] Data were collected only to 2θ of 40°, as the number of significant intensities greatly diminished at higher angles. The intensities of six standard reflections, which were measured after every 100 reflections, decreased slowly with time to about 85% of their original values at the end of data collection. The data were corrected for this decomposition and for absorption.

Standard programs were used to develop and refine this structure.[20,21] On the basis of intensity statistics the centrosymmetric space group $P\bar{1}$ was assumed to be correct. From a sharpened, origin-removed Patterson map the positions of the two independent ruthenium atoms and the bridging oxygen atom were obtained. The remainder of the structure was extracted from cycles of structure factor and electron density calculations. Both *p*-cresol groups appeared to be ill-defined in the maps, although the basic structure of a ring was apparent for each group. Owing to the large number of atoms, only an isotropic refinement was carried out with the eight phenyl and two *p*-cresol rings being treated as rigid groups.[22] The hydrogen coordinates, except for the methyl hydrogen atoms of the *p*-cresol rings, were calculated with a C–H bond length of 0.95 Å and with $B_H = B_C + 1.0$ Å^2 and were added as fixed contributions to the structure factors. The final full-matrix least-squares refinement cycle on F^2, involving all 7630 data and 335 variable parameters, which included isotropic refinement of the nongroup atoms and individual isotropic thermal parameters for the ten rigid groups, gave R and R_w values on F^2 of 0.177 and 0.207, respectively. The high thermal parameters obtained for one of the phenyl groups and for both *p*-cresol rings may indicate some disorder of these rings, consistent with data fall-off at high 2θ. The final difference electron density map has maximum peak heights of ~3 e/Å^3, which are noise peaks near the ruthenium atoms and represent about 5% of the electron density of these atoms on earlier maps. Some smaller peaks of ~1.4 e/Å^3 are located near one *p*-cresol ring; these peaks are

(20) Corfield, P. W. R.; Doedens, R. J.; Ibers, J. A. *Inorg. Chem.* **1967**, *6*, 197–204.
(21) Waters, J. M.; Ibers, J. A. *Inorg. Chem.* **1977**, *16*, 3273–3277.
(22) La Placa, S. J.; Ibers, J. A. *Acta Crystallogr.* **1965**, *18*, 511–519.

Table I. Crystal Data and Data Collection Procedures for Ru(TPP)(p-$OC_6H_4CH_3$)]$_2$O (**2c**) and Ru(TPP)(OEt)(EtOH)·2EtOH (**10**)

	compd **2c**	compd **10**
formula	$C_{102}H_{70}N_8O_3Ru_2$	$C_{52}H_{51}N_4O_4Ru$
formula wt, amu	1657.89	897.08
space group	C_i^1-$P\bar{1}$	C_i^1-$P\bar{1}$
a, Å	16.911 (11)	9.894 (4)
b, Å	19.802 (12)	12.946 (6)
c, Å	12.979 (8)	9.758 (5)
α, deg	99.96 (3)	112.06 (2)
β, deg	104.31 (2)	94.12 (2)
γ, deg	77.53 (2)	71.85 (2)
vol, Å^3	4079	1099
Z	2	1
temp, °C	−157[a]	−160
density (calcd), g/cm^3	1.349	1.355
crystal planes	{0$\bar{1}$1}, (0.290),[b] {10$\bar{1}$}, (0.120), {110}, (0.170)	{010}, (0.110), {01$\bar{1}$}, (0.127), {10$\bar{1}$}, (0.182)
crystal vol, mm^3	0.0074	0.0043
radiation	graphite monochromated Mo Kα, λ(Kα_1) = 0.7093 Å	graphite monochromated Mo Kα, λ(Kα_1) = 0.7093 Å
linear abs coeff, cm^{-1}	4.18	3.97
transmission factors	0.93–0.96[c]	0.95–0.97[d]
detector aperture	6.0 mm wide, 6.5 mm high, 32 cm from crystal	6.0 mm wide, 6.5 mm high, 32 cm from crystal
take-off angle, deg	3.2	3.5
scan speed, deg/min in 2θ	2	2
2θ limits	3.4° < 2θ < 40°	3.4° ≤ 2θ ≤ 55°
background counts	10 s at each end of scan with rescan option; increased to 20 s for 2θ > 33.5°	10 s at each end of scan, with rescan option; increased to 20 s for 2θ > 46°
scan range	1.0° below Kα_1 to 1.0° above Kα_2	1.3° below Kα_1 to 1.0° above Kα_2
data collected	$\pm h,\pm k,+l$	$\pm h,\pm k,+l$
unique data	7630	5073
unique data, with $F_o^2 > 3\sigma(F_o^2)$	4416	3526
$R(F)$, ($F_o^2 > 3\sigma(F_o^2)$)	0.099	0.062
$R_w(F)$, ($F_o^2 > 3\sigma(F_o^2)$)	0.098	0.058
$R(F^2)$	0.177[e]	0.106[e]
$R_w(F^2)$	0.207	0.126
error in observation of unit weight, e^2	1.94	1.24

[a] The low-temperature system is based on a design by Huffman, J. C., Ph.D. Thesis, Indiana University, 1974. [b] The numbers in parentheses are the distances in mm between the Friedel pairs of the preceding form. [c] A Gaussian grid of 4 × 4 × 4 was used for the absorption correction. [d] No absorption correction was necessary. [e] Final refinement done on F^2, using all the data.

between 22 and 35% of the electron density of typical light atoms on a previous map and may result from disorder of this ring.

The final positional and thermal parameters for the nongroup atoms appear in Table **II**,[23] while Table **III**[23] contains group parameters for the eight phenyl and two p-cresol rings. Table **IV**[23] lists structure amplitudes 10|F_o| vs. 10|F_c|, with a negative entry indicating $F_o^2 < 0$.

X-ray Data Collection and Structure Solution for Ru(TPP)(OEt)(EtOH)·2EtOH (10). Suitable crystals of Ru(TPP)(OEt)(EtOH)·2EtOH (**10**) were grown from a solution of 1,2-dichloroethane and ethanol. Since the crystals lose solvent upon exposure to air at room temperature, they were mounted in glass capillaries for the preliminary camera work. Precession photographs taken with Cu Kα radiation revealed only the required center of symmetry, consistent with the space groups $P1$ and $P\bar{1}$. The crystal used for data collection was a dark-purple rhomboidal plate with well-formed faces. At −160 °C, the lattice parameters are a = 9.894 (4) Å, b = 12.946 (6) Å, c = 9.758 (5) Å, α = 112.06 (2)°, β = 94.12 (2)°, and γ = 71.85 (2)°. These were determined by the least-squares analysis of the setting angles for 18 reflections in the range 15 < 2θ < 23° (Mo Kα_1).

Intensity data were collected by standard techniques.[20,21] During the course of data collection, six standard reflections were measured every 100 reflections with no indication of crystal decomposition. Crystal and physical data for this compound appear in Table I.

The structure was solved in space group $P\bar{1}$, which imposes an inversion center on the molecule. An electron density map based on Ru at 0,0,0 revealed the positions of all non-hydrogen atoms of the porphyrin, including both phenyl groups and the coordinated ethanol ligand. A subsequent difference electron density map revealed the presence of an ethanol solvent molecule. Isotropic refinement of this model gave values for R and R_w of 0.12 and 0.13, respectively. The solvent ethanol molecule appears to be disordered between two sites, with oxygen and carbon atoms common to both sites. Figure 1 shows the model of this disorder, along with the atom labeling scheme. Only the occupancy factor (α) of atom CA(2) was allowed to vary, with the occupancy of the CA(2′) position being related to it by 1 − α. The occupancy factors for O(2) and

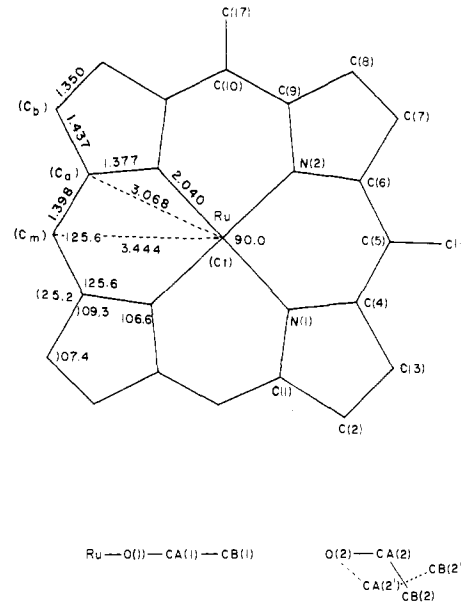

Figure 1. Labeling scheme used for Ru(TPP)(OEt)(EtOH)·2EtOH. Bond parameters have been averaged, assuming D_{4h} symmetry. The nomenclature Ct, C_a, C_b, and C_m is that of Hoard in ref 18a. Hydrogen atoms are named according to the attached carbon atom.

CB(2) were fixed at 1.0. The CB(2) atom was refined as one atomic site, although the model for the disorder places two atoms at this position. Hence atom CB(2′) is not included in the refinement. After a cycle of anisotropic refinement of the nongroup atoms, the hydrogen atom positions of the porphyrin, phenyl groups, and carbon atoms of the coordinated ethanol molecule were found in a difference map. The hydrogen atom contributions to the structure factors were then calculated with a

(23) Supplementary Data.

Scheme I

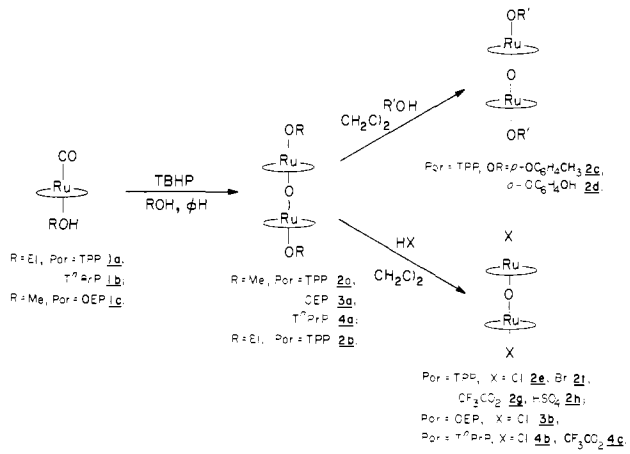

C–H bond length of 0.95 Å and $B_H = B_C + 1.0$ Å^2. Owing to the disorder problem, the hydrogen atoms of the ethanol solvent and the hydroxyl hydrogen of the coordinated ethanol molecule were not idealized. The final full-matrix least-squares refinement cycle was carried out on F^2 and involved all 5075 unique reflections (including those with $F^2 < 0$). The 203 variable parameters included anisotropic refinement for the nongroup atoms and individual, variable isotropic thermal parameters for the two rigid phenyl groups (D_{6h} symmetry, C–C = 1.392 Å). Final values for R and R_w (on F^2) of 0.106 and 0.126 were obtained. The occupancy factor for atom CA(2) is 0.52 (1). The largest peaks on the final difference electron density map (maximum peak height of 1.4 (2) e/Å^3) appear in the vicinity of the phenyl carbon atoms and probably result from the rigid-body refinement of these two rings. A peak height of 1.1 (2) e/Å^3 occurs near atom CB(2) and may result from inadequacies in the model for solvent disorder.

The final positional and thermal parameters of the nongroup atoms are listed in Table V,[23] while Table VI[23] contains group parameters for the phenyl rings. The root-mean-square amplitudes of thermal vibration are found in Table VII.[23] The values of $10|F_o|$ vs. $10|F_c|$ are listed in Table VIII.[23]

Results and Discussion

Preparation and Characterization of the Dinuclear μ-Oxo Ruthenium(IV) Complexes [Ru^{IV}(Por)X]$_2$O. The insertion of ruthenium into the free-base porphyrins H_2(TPP), H_2(OEP), and H_2(T-*n*-PrP) was carried out by a modification of literature methods.[3,13,24] Oxidation by TBHP of the resulting metalloporphyrins Ru(Por)(CO)(ROH) (R = Et, Por = TPP (**1a**), T-*n*-PrP (**1b**); R = Me, Por = OEP (**1c**)) in benzene/ROH solution is developed as a general route to the complexes [Ru^{IV}(Por)(OR)]$_2$O (R = Me, Por = TPP (**2a**), OEP (**3a**), T-*n*-PrP (**4a**); R = Et, Por = TPP (**2b**)). These air-stable compounds are purified by chromatography on silica gel followed by recrystallization from CH_2Cl_2/ROH. The mechanism of the oxidation was not investigated closely, although gas chromatographic analysis indicated that CO is produced.

These complexes undergo facile exchange of the anionic ligand in the presence of an acid catalyst. Alkoxide congeners are synthesized by recrystallization of **2a** or **2b** from CH_2Cl_2 in the presence of alcohols such as *p*-cresol or catechol to yield [Ru(TPP)(OR)]$_2$O (R = *p*-$OC_6H_4CH_3$ (**2c**), *o*-OC_6H_4OH (**2d**)). The alkoxide ligands may also be replaced by treatment of the complexes with a strong acid, HX. In this way the complexes [Ru(Por)X]$_2$O (Por = TPP, X$^-$ = Cl$^-$ (**2e**), Br$^-$ (**2f**), $CF_3CO_2^-$ (**2g**), HSO_4^- (**2h**); Por = OEP, X$^-$ = Cl$^-$ (**3b**); Por = T-*n*-PrP, X$^-$ = Cl$^-$ (**4b**), $CF_3CO_2^-$ (**4c**)) were prepared (Scheme I).

Satisfactory elemental analyses were obtained for all these derivatives, and the molecular weights of **2g** and **3a** were determined in solution. The field desorption mass spectrum of **2g** was recorded in the molecular ion region. Moderate signals in the 1660–1676 m/z range were observed, corresponding closely to the theoretical distribution for the molecular ion species.

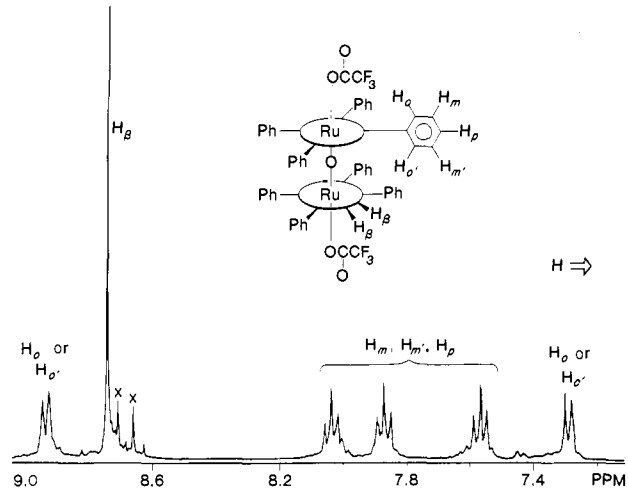

Figure 2. ^{1}H NMR spectrum (360 MHz) of [Ru(TPP)(O_2CCF_3)]$_2$O (**2g**) ($CDCl_2$).

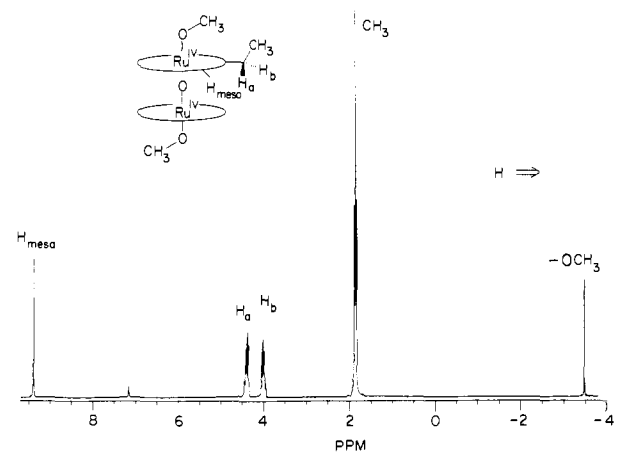

Figure 3. ^{1}H NMR spectrum (360 MHz) of [Ru(OEP)(OMe)]$_2$O (**3a**) (C_6D_6).

The magnetic susceptibility of the μ-oxo Ru(IV) complex **2a** was determined by the Faraday method. The value obtained for χ_M, -7.87×10^{-4} cgs units, is in the range expected for a diamagnetic metalloporphyrin.[18a]

The Ru(IV) μ-oxo dinuclear complexes give well-resolved ^{1}H NMR spectra with resonances in the range expected for diamagnetic metalloporphyrins.[18a] The chemical shifts, measured from 25 to 80 °C for **3a**, are not temperature dependent over this range.

The Ru(IV) TPP derivatives exhibit first-order ^{1}H NMR spectra at 360 MHz. The aromatic region of the 360-MHz ^{1}H NMR spectrum of **2g** is shown in Figure 2. The β-pyrrolic protons give a sharp singlet at 8.74 ppm. Five multiplets are seen to arise from the five *meso*-phenyl protons. On the basis of decoupling experiments and consideration of the porphyrin ring current, the doublets are assigned to the ortho protons and the three triplets to the meta and para protons. The existence of distinct resonances for each of the phenyl protons is consistent with the observed slow rotation of the phenyl rings at 25 °C[25] and also indicates that each side of a phenyl ring exists in a different magnetic environment.

In the OEP series the magnetic nonequivalence of the two sides of the porphyrin plane is manifested in the diastereotopic nature of the ethyl methylene protons. Figure 3 shows the 360-MHz

(24) For Por = TPP an impurity, identified by a visible band near 600 nm and presumed to be a chlorin, was generated during the insertion process. The product was purified by an oxidative process based on that described in ref 18b.

(25) (a) Eaton, S. S.; Eaton, G. R. *J. Chem. Soc., Chem. Commun.* **1974**, 576–577. (b) Eaton, G. R.; Eaton, S. S. *J. Am. Chem. Soc.* **1975**, *97*, 235–236. (c) Eaton, S. S.; Eaton, G. R. *Ibid.* **1977**, *99*, 6594–6599.

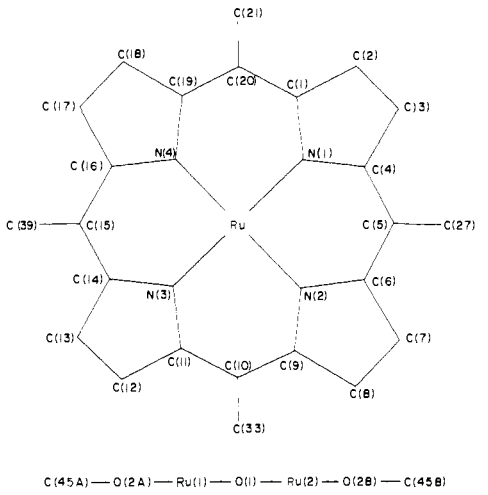

Figure 4. Labeling scheme used for $[Ru(TPP)(p\text{-}OC_6H_4CH_3)]_2O$. The two macrocycles of the molecule are identically numbered and are distinguished by the letters A and B in the text.

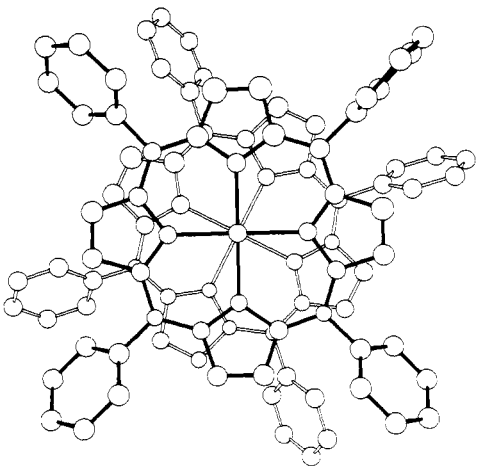

Figure 6. Drawing of the $[Ru(TPP)(p\text{-}OC_6H_4CH_3)]_2O$ molecule viewed down the Ru–O–Ru axis. Non-hydrogen atoms are drawn with 50% probability ellipsoids. All carbon atoms of phenyl rings are drawn with isotropic thermal parameters set equal to 3.0 Å^2. Hydrogen atoms are labeled according to the attached carbon atom and are omitted for clarity here.

^{1}H NMR spectrum of $[Ru(OEP)(OMe)]_2O$ (**3a**). Two multiplets (4.37, 3.99 ppm) arise from the two magnetically distinguishable protons of the methylene group.

The upfield shifts of the alkoxide ligand resonances, relative to those for the free alcohols, are attributed to the porphyrin ring current effect.[18a] In the absence of an acid catalyst, axial ligand exchange is slow on the NMR time scale. For the alkoxide derivatives the relative intensities of the NMR peaks are consistent with a 1:1 ratio of axial ligand to porphyrin, further substantiating the proposed stoichiometry.[26]

Electronic spectral data (700–350 nm) were recorded for these complexes. The alkoxide derivatives of the TPP series exhibit a broad band near 550 nm with a shoulder at ca. 530 nm. TPP complexes in which the anionic axial ligand is the conjugate base of a strong acid show an additional strong band close to 587 nm with a shoulder near 564 nm.

The dinuclear nature of these complexes is demonstrated by molecular weight and mass spectral measurements. The magnetic nonequivalent of the two sides of the porphyrin plane is also consistent with a dinuclear formulation. Characterization of the Ru(IV) μ-oxo complexes is completed and the dinuclearity confirmed by an X-ray crystal structure determination of $[Ru(TPP)(p\text{-}OC_6H_4CH_3)]_2O$ (**2c**).

The numbering scheme used to describe both macrocycles of $[Ru(TPP)(p\text{-}OC_6H_4CH_3)]_2O$ (**2c**) is shown in Figure 4. Each macrocycle is distinguished by the letters A or B; atom Ru(1) is in the A half of the molecule while atom Ru(2) is in the B half. Individual bond lengths and angles, along with values averaged in accordance with D_{4d} symmetry, are listed in Table IX. The limited size of the data set along with isotropic refinement and probable disorder in some parts of the structure results in large errors for these structural parameters and a wide variation of values for a particular bond type. Averaging these values gives a reasonable geometry for the porphyrin core. Figure 5[23] displays the packing of this molecule in the unit cell.

A comparison of some of the structural features of $[Ru(TPP)(p\text{-}OC_6H_4CH_3)]_2O$ (**2c**) with those of the porphyrin dimers $[Fe(TPP)]_2O$,[27] $[Fe(TPP)]_2N$,[28] and $[Ru(OEP)(OH)]_2O$[17] is presented in Table X. The Ru–O–Ru angle of **2c** is 177.8 (7)° so that the mean planes through the two 24-atom porphyrinato cores are not parallel. The dihedral angle between these planes is 2.5°. The $[Ru(TPP)]_2O$ unit, viewed down the Ru–O–Ru axis in Figure 6, shows the staggering of these planes with respect to each other. The N–Ru–Ru*–N* torsion angle of 27.9° is consistent with angles observed in the other porphyrin dimers. The 3.8-Å interplanar distance between the porphyrinato cores in compound **2c** is approximately the same as that observed in $[Ru(OEP)(OH)]_2O$, 3.7 Å. However, both these separations are much smaller than those observed in the iron porphyrin dimers, perhaps because the displacement of the metal atom from the porphyrinato core is much larger for the iron than for the ruthenium dimers.

It is interesting that the Ru–O bond length of 1.789 (11) Å in the μ-oxo bridge of compound **2c** is probably not significantly different from the 1.847 (13) Å value in $[Ru(OEP)(OH)]_2O$.[17] However, the Ru–O(2) distance here of 1.944 (11) Å is significantly shorter than the 2.195 (26) Å value for the Ru–O(H) bond of the hydroxo complex. This may be an indication of substitution problems in this compound (see below). Further comparisons between these two ruthenium dimers are difficult to make owing to the large standard deviations in the bond lengths and angles for both structures.

Table XI[23] contains some least-squares planes through molecule **2c**. The ruthenium atom is about 0.07 Å out of the N_4 plane in the direction of the μ-oxo bridge. The deviations of the atoms from the mean plane through the porphyrinato core are much larger for compound **2c** than for $[Ru(OEP)(OH)]_2O$. The puckering of **2c** is such that a pseudo-2-fold rotation axis exists along the Ru–O–Ru bond axis. The dihedral angles between the phenyl groups and the least-squares porphyrinato planes are in the range 43–70°, except for the C(33A) phenyl group which is at an angle of ~92°. It is this phenyl group that displays large thermal parameters.

Masuda et al. recently reported the crystal structure of $[Ru^{IV}(OEP)(OH)]_2O{\cdot}2CH_3OH$.[17] For both this μ-oxo hydroxide derivative and the Ru(IV) μ-oxo alkoxide series reported herein, Ru(III) would be distinguished from Ru(IV) by the presence or absence of a proton on the hydroxo or alkoxo axial ligand to form aquo or alcohol ligands. Neither crystal structure is capable of resolving such protons. However, the series of species $[Ru(Por)X]_2O$ (**2e–h**, **3b**, **4b–c**), where X is the conjugate base of a strong acid, clearly demonstrates the +IV oxidation state of the ruthenium center. The alkoxo complexes can be transformed into derivatives of the second series simply upon treatment with acid. This process does not involve electron transfer and hence there is no change in oxidation state. The results of two X-ray crystal structure analyses of $[Ru(OEP)Cl]_2O$ (**3b**) confirm this stoichiometry. The complex exhibits a crystallographically imposed linear oxo bridge with a Ru–O bridge distance of 1.79 Å and a Ru–Cl bond length of 2.32 Å.[29] One further formulation for these

(26) Exchange of alkoxide ligand with trace quantities of water in NMR solvents was occasionally observed. In order to observe the full complement of ligand protons upon integration, some spectra were recorded in the presence of a small quantity of the corresponding alcohol.

(27) Hoffman, A. B.; Collins, D. M.; Day, V. W.; Fleischer, E. B.; Srivastava, T. S.; Hoard, J. L. *J. Am. Chem. Soc.* **1972**, *94*, 3620–3626.

(28) Scheidt, W. R.; Summerville, D. A.; Cohen, I. A. *J. Am. Chem. Soc.* **1976**, *98*, 6623–6628.

complexes that should be considered is a Ru(III) porphyrin radical cation $[Ru^{III}(Por^{+\cdot})X]_2O$. The observed diamagnetism is inconsistent with such a radical species.

A comparison of the report by Masuda et al. of the synthesis and structure of $[Ru(OEP)(OH)]_2O$[17] with our own work on this and related species yields some interesting observations. The complex of Masuda et al. was synthesized by oxidation with TBHP of Ru(OEP)(CO)L in benzene, followed by recrystallization from CH_2Cl_2/CH_3OH. In our hands preparation of the same complex by reaction of the metal–metal bonded Ru(II) dimer $[Ru(OEP)]_2$ with O_2 in benzene,[5] followed by recrystallization from CH_2Cl_2/CH_3OH, yields the methoxide congener $[Ru(OEP)(OMe)]_2O$ (**3a**). We have observed these complexes to be somewhat hygroscopic and to possess readily exchangeable axial ligands. By elemental analysis the formulation reported by Masuda et al. $[Ru(OEP)(OH)]_2O\cdot 2CH_3OH$ would be indistinguishable from the aquo solvate of **3a**, $[Ru(OEP)(OMe)]_2O\cdot 2H_2O$. Further discrepancies between our work and that of Masuda et al. arise upon comparison of the electronic spectra of these species. They report visible bands at 512 and 580 nm for the hydroxo complex in CH_2Cl_2. However, we have recorded bands at 512 and 565–570 nm for our hydroxo species (prepared by the alternative synthetic route[5]) and bands at 512 and 580 nm for the methoxo complex **3a** in 5% CH_3OH/CH_2Cl_2. These data suggest that the complex prepared by Masuda et al., at least in solution, may be predominantly the methoxide-substituted species.

Several comparisons may be made between the Ru(IV) μ-oxo complexes reported herein and other transition-metal oxo complexes, especially those from the same triad. High oxidation state monomeric metalloporphyrins that bear an oxo ligand and contain the transition elements Ti,[30] V,[31] Cr,[32] Mn,[33] and Mo[34] have been synthesized and characterized structurally. These complexes can be handled at ambient temperatures. In contrast it is necessary to employ cryogenic techniques and hindered porphyrin ligands to stabilize the highly reactive ferryl complexes.[35,36] It has been shown that the ferryl species readily undergo bimolecular reactions to form Fe(III) μ-oxo dinuclear complexes.[36,37] A monomeric ruthenyl complex that contains a porphyrin ligand has not yet been made, although Meyer and co-workers have prepared the Ru(IV) complexes $[(bpy)_2(py)Ru{=}O]^{2+}$ and $[(bpy)(trpy)Ru{=}O]^{2+}$ by chemical or electrochemical oxidation of the corresponding Ru(II) aquo species.[38] They have also studied Ru(IV) μ-oxo complexes in the same system. Oxidation of $\{[(bpy)_2Ru^{III}Cl]_2O\}^{2+}$ by one or two electrons yields the mixed-valent and Ru(IV)–Ru(IV) dinuclear species, respectively. The oxo bridge remains intact.[39] Complexes of Ru(VI) that contain two oxo ligands are much better known than the monooxo Ru(IV) species. Representative compounds $[RuO_2(NH_3)_4]Cl_2$ and $RuO_2(py)_2Cl_2$ are diamagnetic and contain the trans O=Ru=O moiety.[40]

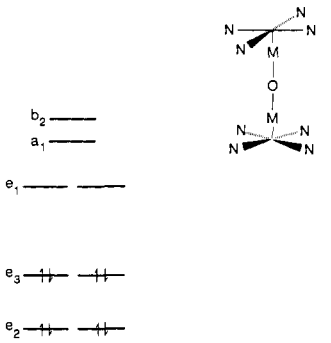

Figure 7. d-Orbital ordering and electron configuration for a $(MN_4)_2O$ model.[44] The electron configuration is shown for a d^4 metal, such as Ru(IV).

In iron porphyrin chemistry the Fe^{III} μ-oxo complexes (Por)-Fe^{III}-O-Fe^{III}(Por) are significant as the products of irreversible oxidation of Fe(II) dioxygen species.[27,37] No ruthenium analogue of these species bearing a porphyrin ligand is known, although Weaver et al. have reported several such compounds containing bipyridyl ligands.[39] Conversely, there are no Fe(IV) μ-oxo species known. The complex $\{[Fe(TPP)]_2O\}[ClO_4]_2$ was originally thought to be such a species but was later reformulated as an Fe(III) porphyrin radical cation.[41]

In characterizing the products of oxidation reactions, especially the high oxidation state porphyrin complexes presented herein, the profound effect of axial ligation on redox site must be considered. For example, although no Fe(IV) μ-oxo species are known, the monomeric oxo complex Fe(TPP)(O)(1-MeIm) contains Fe(IV).[36] The lack of an oxo ligand in $[Ru(OEP)(P\text{-}n\text{-}Bu_3)_2]^{2+}$ may have a similar profound effect on the site of oxidation. This complex, prepared by electrochemical oxidation of the corresponding Ru(II) or Ru(III) species, is formally a "Ru(IV) equivalent" but has been formulated as the Ru(III) porphyrin radical cation.[42] The nature of the metal center is also an important factor, even within the same triad. For example, one-electron oxidation of $M^{II}(OEP)(CO)$ yields reversible oxidation at the metal site for M = Os, reversible porphyrin oxidation for Ru, and irreversible oxidation for Fe.[15]

The first Ru(IV) μ-oxo complex to be reported was $K_4[(RuCl_5)_2O]\cdot H_2O$.[43] The structural characterization of this diamagnetic complex showed that the Ru–O–Ru bridge is linear and that the Ru–O bond length is shorter than expected for a Ru–O single bond. In an analysis of the bonding in this complex, Dunitz and Orgel[43b] considered a molecular orbital scheme that explained the diamagnetism of the complex and suggested the existence of some Ru–O–Ru multiple bond character. More recently Tatsumi and Hoffmann et al.,[44] in their theoretical analysis of bridged porphyrin dimers, developed an ordering for the metal d orbitals of an $(MN_4)_2O$ unit that accounts for both the diamagnetism and the linear bridge observed for the μ-oxo Ru(IV) porphyrin complexes reported herein. The molecular orbitals, based on the metal d orbitals, for an $(MN_4)_2O$ model are shown in Figure 7. The complexes $[Ru^{IV}(Por)X]_2O$ are diamagnetic as 8 d electrons fill the low-lying e_2 and e_3 levels with paired electrons. This contrasts with the monomeric Ru(IV) oxo complex $[(bpy)_2(py)Ru{=}O][ClO_4]_2$ for which $\mu_{eff} = 2.95\ \mu_B$, corresponding to two unpaired electrons as expected for a single paramagnetic six-coordinate

(29) (a) Barnes, C. E.; Santarsiero, B. D.; Raybuck, S. A.; Woo, L. K., unpublished data. (b) Masuda, H.; Taga, T.; Osaki, K.; Sugimoto, H.; Mori, M.; Ogoshi, H. *Bull. Chem. Soc. Jpn.* **1982**, *55*, 3887–3890.

(30) Dwyer, P. N.; Puppe, L.; Buchler, J. W.; Scheidt, W. R. *Inorg. Chem.* **1975**, *14*, 1782–1785.

(31) (a) Pettersen, R. C.; Alexander, L. E. *J. Am. Chem. Soc.* **1968**, *90*, 3873–3875. (b) Molinaro, F. S.; Ibers, J. A. *Inorg. Chem.* **1976**, *15*, 2278–2283.

(32) (a) Budge, J. R.; Gatehouse, B. M. K.; Nesbit, M. C.; West, B. O. *J. Chem. Soc., Chem. Commun.* **1981**, 370–371. (b) Groves, J. T.; Kruper, W. J., Jr.; Haushalter, R. C.; Butler, W. M. *Inorg. Chem.* **1982**, *21*, 1363–1368.

(33) Willner, I.; Otvos, J. W.; Calvin, M. *J. Chem. Soc., Chem. Commun.* **1980**, 964–965.

(34) (a) Ledon, H.; Mentzen, B. *Inorg. Chim. Acta* **1978**, *31*, L393–L394. (b) Diebold, T.; Chevrier, B.; Weiss, R. *Inorg. Chem.* **1979**, *18*, 1193–1200.

(35) Groves, J. T.; Haushalter, R. C.; Nakamura, M.; Nemo, T. E.; Evans, B. J. *J. Am. Chem. Soc.* **1981**, *103*, 2884–2886.

(36) Chin, D.-H.; Balch, A. L.; La Mar, G. N. *J. Am. Chem. Soc.* **1980**, *102*, 1446–1448.

(37) (a) Chin, D.-H.; Del Gaudio, J.; La Mar, G. N.; Balch, A. L. *J. Am. Chem. Soc.* **1977**, *99*, 5486–5488. (b) Chin, D.-H.; La Mar, G. N.; Balch, A. L. *Ibid.* **1980**, *102*, 4344–4350.

(38) (a) Moyer, B. A.; Meyer, T. J. *J. Am. Chem. Soc.* **1978**, *100*, 3601–3603. (b) Moyer, B. A.; Thompson, M. S.; Meyer, T. J. *Ibid.* **1980**, *102*, 2310–2312.

(39) Weaver, T. R.; Meyer, T. J.; Adeyemi, S. A.; Brown, G. M.; Eckberg, R. P.; Hatfield, W. E.; Johnson, E. C.; Murray, R. W.; Untereker, D. *J. Am. Chem. Soc.* **1975**, *97*, 3039–3048.

(40) Pawson, D.; Griffith, W. P. *Chem. Ind. (London)* **1972**, *Aug 5*, 609.

(41) (a) Phillippi, M. A.; Goff, H. M. *J. Am. Chem. Soc.* **1979**, *101*, 7641–7643. (b) Shimomura, E. T.; Phillippi, M. A.; Goff, H. M.; Scholz, W. F.; Reed, C. A. *Ibid.* **1981**, *103*, 6778–6780.

(42) Barley, M.; Becker, J. Y.; Domazetis, G.; Dolphin, D.; James, B. R. *J. Chem. Soc., Chem. Commun.* **1981**, 982–983.

(43) (a) Mathieson, A. McL.; Mellor, D. P.; Stephenson, N. C. *Acta Crystallogr.* **1952**, *5*, 185–186. (b) Dunitz, J. D.; Orgel, L. E. *J. Chem. Soc.* **1953**, 2594–2596.

(44) (a) Tatsumi, K.; Hoffmann, R. *J. Am. Chem. Soc.* **1981**, *103*, 3328–3341. (b) Tatsumi, K.; Hoffmann, R.; Whangbo, M.-H. *J. Chem. Soc., Chem. Commun.* **1980**, 509–511.

Table IX. Distances (Å) and Angles (deg) in $[Ru(TPP)(p\text{-}OC_6H_4CH_3)]_2O$ (2c)

	ring A	ring B		ring A	ring B
Ru–O(1)	1.787 (11)	1.791 (11)	Ru–N(1)–C(1)	126.3 (11)	125.6 (11)
	av 1.789 (11)[a]		Ru–N(1)–C(4)	126.1 (11)	125.4 (11)
Ru–O(2)	1.942 (10)	1.947 (11)	Ru–N(2)–C(6)	125.3 (12)	124.1 (12)
	av 1.944 (11)		Ru–N(2)–C(9)	125.9 (12)	125.5 (12)
O(2)–C(45)	1.338 (19)	1.361 (23)	Ru–N(3)–C(11)	126.4 (12)	125.1 (12)
	av 1.347 (23)		Ru–N(3)–C(14)	125.3 (11)	126.6 (12)
Ru–N(1)	2.039 (13)	2.064 (13)	Ru–N(4)–C(16)	125.6 (11)	125.4 (11)
Ru–N(2)	2.060 (14)	2.056 (14)	Ru–N(4)–C(19)	125.7 (11)	127.3 (11)
Ru–N(3)	2.041 (13)	2.039 (14)	av Ru–N–C_a	125.7 (12)	
Ru–N(4)	2.057 (13)	2.048 (13)	N(1)–C(1)–C(2)	110.1 (15)	108.5 (14)
av Ru–N	2.050 (14)		N(1)–C(4)–C(3)	108.9 (15)	108.0 (14)
N(1)–C(1)	1.361 (19)	1.383 (17)	N(2)–C(6)–C(7)	105.4 (16)	107.9 (16)
N(1)–C(4)	1.399 (18)	1.341 (18)	N(2)–C(9)–C(8)	110.2 (17)	106.3 (17)
N(2)–C(6)	1.373 (19)	1.342 (20)	N(3)–C(11)–C(12)	109.2 (16)	106.9 (15)
N(2)–C(9)	1.361 (20)	1.413 (20)	N(3)–C(14)–C(13)	107.8 (15)	109.9 (15)
N(3)–C(11)	1.358 (20)	1.400 (19)	N(4)–C(16)–C(17)	107.1 (15)	109.8 (15)
N(3)–C(14)	1.396 (18)	1.346 (19)	N(4)–C(19)–C(18)	107.5 (15)	109.0 (15)
N(4)–C(16)	1.406 (19)	1.361 (19)	av N–C_a–C_b	108.3 (17)	
N(4)–C(19)	1.372 (19)	1.376 (18)	C(1)–N(1)–C(4)	106.0 (14)	108.9 (14)
av N–C_a	1.375 (23)		C(6)–N(2)–C(9)	108.8 (15)	109.7 (15)
C(1)–C(2)	1.448 (21)	1.419 (20)	C(11)–N(3)–C(14)	107.3 (14)	108.1 (14)
C(4)–C(3)	1.406 (22)	1.440 (21)	C(16)–N(4)–C(19)	108.5 (14)	106.9 (14)
C(6)–C(7)	1.453 (24)	1.454 (22)	av C_a–N–C_a	108.0 (15)	
C(9)–C(8)	1.435 (22)	1.446 (23)	C(1)–C(2)–C(3)	105.8 (16)	106.7 (15)
C(11)–C(12)	1.441 (22)	1.447 (23)	C(4)–C(3)–C(2)	109.1 (16)	107.9 (15)
C(14)–C(13)	1.452 (22)	1.460 (22)	C(6)–C(7)–C(8)	110.6 (18)	108.1 (17)
C(16)–C(17)	1.405 (22)	1.434 (20)	C(9)–C(8)–C(7)	104.8 (18)	108.0 (18)
C(19)–C(18)	1.432 (21)	1.417 (21)	C(11)–C(12)–C(13)	108.1 (17)	109.1 (17)
av C_a–C_b	1.436 (24)		C(14)–C(13)–C(12)	107.7 (16)	105.9 (16)
C(2)–C(3)	1.348 (21)	1.367 (20)	C(16)–C(17)–C(18)	109.0 (16)	106.2 (16)
C(7)–C(8)	1.343 (23)	1.355 (23)	C(19)–C(18)–C(17)	107.7 (16)	108.0 (16)
C(12)–C(13)	1.330 (21)	1.350 (21)	av C_a–C_b–C_b	107.6 (18)	
C(17)–C(18)	1.361 (21)	1.360 (21)	N(1)–C(1)–C(20)	127.0 (16)	125.8 (15)
av C_b–C_b	1.352 (23)		N(1)–C(4)–C(5)	125.1 (16)	128.5 (16)
C(1)–C(20)	1.400 (20)	1.401 (19)	N(2)–C(6)–C(5)	126.6 (18)	129.9 (16)
C(4)–C(5)	1.390 (21)	1.394 (20)	N(2)–C(9)–C(10)	125.3 (18)	125.8 (18)
C(6)–C(5)	1.396 (22)	1.417 (21)	N(3)–C(11)–C(10)	125.3 (17)	126.7 (17)
C(9)–C(10)	1.407 (22)	1.347 (23)	N(3)–C(14)–C(15)	127.2 (16)	125.2 (17)
C(11)–C(10)	1.399 (22)	1.382 (21)	N(4)–C(16)–C(15)	124.4 (16)	126.2 (15)
C(14)–C(15)	1.336 (20)	1.399 (20)	N(4)–C(19)–C(20)	126.9 (15)	125.2 (16)
C(16)–C(15)	1.404 (21)	1.397 (20)	av N–C_a–C_m	126.3 (18)	
C(19)–C(20)	1.394 (20)	1.384 (20)	C(4)–C(5)–C(6)	125.5 (16)	121.1 (16)
av C_a–C_m	1.391 (23)		C(9)–C(10)–C(11)	125.6 (18)	126.3 (18)
C(5)–C(27)	1.498 (22)	1.482 (16)	C(14)–C(15)–C(16)	126.5 (16)	125.5 (16)
C(10)–C(33)	1.509 (22)	1.495 (21)	C(19)–C(20)–C(1)	123.3 (16)	125.8 (15)
C(15)–C(39)	1.495 (20)	1.509 (18)	av C_a–C_m–C_a	124.9 (18)	
C(20)–C(21)	1.497 (17)	1.498 (19)	C(3)–C(4)–C(5)	125.9 (17)	123.4 (16)
av C_m–C_p	1.497 (22)		C(7)–C(6)–C(5)	127.9 (18)	122.2 (17)
Ru(1)–O(1)–Ru(2)	177.8 (7)		C(8)–C(9)–C(10)	124.1 (19)	127.9 (19)
O(1)–Ru–O(2)	177.8 (5)	179.2 (5)	C(12)–C(11)–C(10)	125.5 (18)	126.4 (17)
Ru–O(2)–C(45)	128.4 (8)	132.2 (10)	C(13)–C(14)–C(15)	124.8 (16)	124.3 (17)
O(1)–Ru–N(1)	90.6 (5)	90.8 (5)	C(17)–C(16)–C(15)	128.5 (17)	124.0 (16)
O(1)–Ru–N(2)	91.8 (5)	94.4 (5)	C(18)–C(19)–C(20)	125.5 (16)	125.8 (16)
O(1)–Ru–N(3)	94.2 (5)	92.1 (5)	C(2)–C(1)–C(20)	123.0 (16)	125.7 (15)
O(1)–Ru–N(4)	91.4 (5)	89.6 (5)	av C_b–C_a–C_m	125.2 (19)	
O(2)–Ru–N(1)	87.6 (5)	89.6 (5)	C(4)–C(5)–C(27)	118.8 (13)	120.9 (14)
O(2)–Ru–N(2)	89.5 (5)	86.3 (5)	C(6)–C(5)–C(27)	115.5 (15)	117.9 (13)
O(2)–Ru–N(3)	87.5 (5)	87.5 (5)	C(9)–C(10)–C(33)	118.5 (16)	115.5 (15)
O(2)–Ru–N(4)	87.3 (5)	89.7 (5)	C(11)–C(10)–C(33)	115.7 (14)	118.1 (14)
N(1)–Ru–N(2)	90.3 (5)	90.1 (5)	C(14)–C(15)–C(39)	118.3 (13)	116.9 (14)
N(1)–Ru–N(3)	175.1 (5)	177.1 (5)	C(16)–C(15)–C(39)	114.9 (14)	117.7 (14)
N(1)–Ru–N(4)	89.5 (5)	89.5 (5)	C(19)–C(20)–C(21)	118.1 (14)	117.4 (13)
N(2)–Ru–N(3)	89.9 (5)	90.2 (5)	C(1)–C(20)–C(21)	118.5 (12)	116.8 (12)
N(2)–Ru–N(4)	176.8 (5)	175.9 (5)	av C_a–C_m–C_p	117.5 (16)	
N(3)–Ru–N(4)	90.1 (5)	90.1 (5)			

[a] Average values are weighted; the error is taken as the larger of the unweighted estimated standard deviation of a single observation and that estimated from the inverse least-squares matrix.

Ru(IV) center.[38a] The theoretical analysis shows for $(Fe^{III}N_4)_2O$ that bending of the Fe–O–Fe bridge is favored. It was predicted that a double oxidized $(Fe^{III}N_4)_2O$ unit would have no occupied valence orbital favoring a bent form and the bridge would be linear.[44] This prediction is borne out for the isoelectronic Ru(IV) μ-oxo complexes described here.

It is also stated in the theoretical analysis[44] that "the bridging atom can support strong electronic interactions between the two

Table X. Comparison of Structural Features in Some Porphyrin Dimers

	$[Fe(TPP)]_2O$[a,b]	$[Fe(TPP)]_2N$[c]	$[Ru(OEP)(OH)]_2O$[d]	$[Ru(TPP)(p\text{-}OC_6H_4CH_3)]_2O$[e]
metal–O, Å	1.763 (1)	1.6605 (7)	1.847 (13)	1.789 (11)
M–O–M, deg	174.5 (1)	180[f]	180[f]	177.8 (7)
dihedral angle between porphyrinato cores,[g] deg	3.7	0.0	0.0	2.5
displacement of metal atom from porphyrinato core, Å	0.54	0.41	0.01	0.18; 0.11[g]
displacement of metal atom from least-squares plane through 4 N atoms, Å	0.50	0.32	0.03	0.07; 0.06
distance between porphyrinato cores, Å	4.6	4.2	3.7	3.8
torsion angle: N–M–M*–N*,[h] deg	35.4	31.7	22.7	27.9

[a] All structures were determined at room temperature except for $[Ru(TPP)(p\text{-}OC_6H_4CH_3)]_2O$. [b] Reference 27. [c] Reference 28. [d] Reference 17. [e] This work. [f] Angle is exactly 180°, as required by symmetry. Hence the least-squares planes through the porphyrinato cores in the molecule are parallel. [g] The porphyrinato core is defined here as being the least-squares plane through the 20 carbon atoms and 4 N atoms of the macrocycle. [h] Torsion angle given is the smallest angle defined by the metal–N bond of one porphyrinato core and the metal*–N* bond of the second porphyrinato core.

metal sites so that chemical and physical properties of the dimer may differ substantially from related monomers". The robust, kinetically inert nature of the Ru(IV) oxo bridge illustrates the veracity of this statement. Monomeric ferryl species are so reactive that they must be prepared at low temperatures.[35,36] Both the ferryl species and the monomeric ruthenyl complexes are active catalysts for the oxidation of organic substrates.[35,38] The Ru^{IV}/Ru^{III} couple for $[(bpy)(trpy)Ru^{IV}(O)]^{2+}$ has been measured at 0.57 V vs. Ag/AgCl.[38b] In contrast preliminary electrochemical measurements on $[Ru(OEP)(OMe)]_2O$ in CH_3CN indicate that the first reduction occurs as an irreversible wave at ca. −1 V vs. Ag/AgCl, a surprisingly negative potential for a metal in such a high formal oxidation state.[45] The iron species $[(Fe^{III}(Por)]_2O$ and $[Fe^{III}(Por^{+\cdot})]_2O$ are readily cleaved by strong acids HX.[41] The Ru(III) complexes $\{[(bpy)_2RuCl]_2O\}^{2+}$ are cleaved by acid, but these dinuclear species are poor oxidants compared with monomeric Ru(III) bis-bipyridyl systems.[39] We have observed that strong acids appear to have no effect on the oxo bridge of the Ru(IV) complexes reported here, instead serving only to substitute the axial anionic ligand. These observations support the premise that the dinuclear nature of the Ru(IV) μ-oxo oligomers is a key factor in determining the chemical reactivity.

The mechanism of formation of the μ-oxo Ru(IV) species was not investigated. It is interesting to speculate, however, on the possible role of ruthenyl intermediates that may be formed by oxygen atom transfer from TBHP. The formation of ferryl species by oxygen atom transfer[35,46] and the involvement of ferryls in μ-oxo formation[36,37] have been demonstrated. In contrast, the route to the monomeric ruthenyl species developed by Meyer et al. has the potential oxo moiety already in place, coordinated as an aquo ligand.[38] These pyridyl ruthenyl complexes are apparently kinetically inert toward μ-oxo formation, although further studies show that such oligomers can be isolated.[39]

Our interest in the interaction of dioxygen with ruthenium(II) porphyrins led us to find a route to such complexes bearing labile axial ligands. The Ru(IV) μ-oxo dinuclear complexes described herein can be reduced by sodium borohydride to give monomeric ruthenium(II) porphyrins. Reduction of $[Ru(TPP)(OEt)]_2O$ (**2b**) by $NaBH_4$ in THF solution under an argon atmosphere affords the complex $Ru(TPP)(THF)_2$ (**5**). Sodium dithionite was also found to be a suitable reducing agent. Other bis-ligand complexes $Ru(TPP)L_2$ could be prepared by recrystallization of **5** in the presence of ligands L such as MeCN, pyridine, PPh_3, or imidazole. However, some difficulties in the preparation of analytically pure samples were encountered, as the presence of any potentially coordinating species leads to mixtures of substituted products. Treatment of the Ru(IV) μ-oxo complexes, **2b**, or $[Ru(T\text{-}n\text{-}PrP)(OMe)]_2O$ (**4a**) with PPh_3 in refluxing benzene gives rise to reduction of the dinuclear species and production of triphenylphosphine oxide. However, this reaction is not synthetically useful as the Ru(II) products, $Ru(Por)(PPh_3)_2$ (Por = TPP (**6a**), T-*n*-PrP (**6b**)), contain PPh_3 ligands that are not easily substituted.

Scheme II

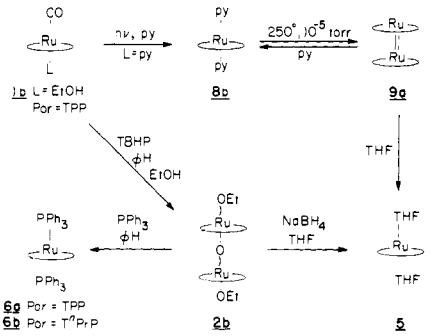

Photochemical ejection of the CO moiety in the presence of pyridine or other strongly coordinating ligands has been utilized as a route to bis-ligand Ru(II) porphyrin complexes.[4b,12,14b] However, there still remains the difficulty of substituting these strongly bound ligands with more labile ligands (alcohols, THF) or ligands of biological significance (thiols, imidazoles). We followed a procedure based on that of Antipas et al.[12] and found that irradiation of Ru(Por)(CO)L (L = py, Por = TPP (**7a**), OEP (**7b**); L = EtOH, Por = T-*n*-PrP (**1b**)) in refluxing pyridine followed by reduction of the solvent volume affords, in high yield, $Ru(Por)(py)_2$ (Por = TPP (**8a**), OEP (**8b**), T-*n*-PrP (**8c**)). Pyrolysis of **8a** or **8b** at 250 °C and 10^{-5} torr for several hours removes the pyridine ligands, and the metal–metal bonded dimers $[Ru(TPP)]_2$ (**9a**) or $[Ru(OEP)]_2$ (**9b**) are formed. We recently reported the characterization of these novel species.[5,14] Treatment of a benzene or toluene solution of **9a** or **9b** with any potential ligand L, such as pyridine, imidazole, or THF, yields the monomeric $Ru(Por)L_2$ complexes in quantitative yield (based on the ruthenium carbonyl precursor).[5] We have found this to be the most convenient route to ruthenium(II) complexes bearing a wide variety of axial ligands.

Ruthenium(II) porphyrin complexes that contain strongly coordinating axial ligands (py, PPh_3) can be handled in air, but the derivatives with more labile ligands must be manipulated under anaerobic conditions. One ligand L in the complexes $Ru(Por)L_2$ is labile with respect to replacement by CO. The substitution takes place on bubbling CO through a solution of the complex. The carbonyl products, Ru(Por)(CO)L, can be identified by a band in the visible spectrum at ca. 530 nm and an IR absorption at ca. 1960 cm^{-1} for the TPP series. This reaction demonstrates the high affinity of Ru(II) porphyrins for the CO ligand. There is precedent for this high affinity in iron porphyrin chemistry.[47]

(45) Our preliminary experiments indicated that the electrochemistry of these species is complex, and it was not investigated in detail.

(46) Groves, J. T.; Nemo, T. E.; Myers, R. S. *J. Am. Chem. Soc.* **1979**, *101*, 1032–1033.

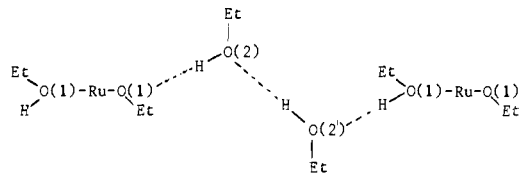

Figure 9. Hydrogen-bonding scheme for Ru(TPP)(OEt)(EtOH)·2EtOH (**10**).

The preparation and substitution chemistry of the ruthenium(II) porphyrins is summarized in Scheme II.

Interactions of Ruthenium Porphyrin Complexes with Dioxygen. We recently communicated the results of our studies on the reaction of oxygen with the metal–metal bonded dimers $[Ru(TPP)]_2$ (**9a**) and $[Ru(OEP)]_2$ (**9b**).[5] Exposure of a benzene solution of **9b** to oxygen results in rapid, irreversible oxidation with clean isosbestic behavior. The product was identified as the μ-oxo Ru(IV) complex $[Ru(OEP)(OH)]_2O$ (**3c**). All the proton resonances expected for this species were observed in the ^1H NMR spectrum. Reaction of a methanol solution of **3c** with aqueous HCl affords the chloro-substituted congener $[Ru(OEP)Cl]_2O$ (**3b**). This compound has been synthesized by the alternative route described above. Similar behavior is observed for the TPP derivative $[Ru(TPP)]_2$ (**9a**).[5]

The Ru(II) tetrahydrofuran complex $Ru(TPP)(THF)_2$ (**5**) in dichloromethane solution undergoes a very rapid oxidation when exposed to oxygen. The product, after recrystallization from CH_2Cl_2/ethanol, is the dinuclear Ru(IV) ethoxide complex **2b**. However, if a solution of **5** in dichloromethane/ethanol (1:1) is exposed to oxygen, a rapid reaction ensues, but UV–visible spectroscopy indicates that the product **10** is different from $[Ru(TPP)(OEt)]_2O$ (**2b**). Compound **10**, distinguishable by a band at 518 nm in the visible spectrum, can be crystallized from dichloromethane/ethanol. When the crystals are redissolved in ethanol/dichloromethane in air, or in CH_2Cl_2 in the absence of air, the resulting solutions have the same electronic spectrum as the original solution in which **10** was produced. However, a solution of **10** in CH_2Cl_2 alone reacts with oxygen to form the μ-oxo complex **2b**.

Complex **10** was characterized by an X-ray structure determination. The basic composition is $Ru^{III}(TPP)(OEt)(EtOH)$·2EtOH. However, this axial ligand formulation of $Ru^{III}(OEt)(EtOH)$ differs by only one hydrogen atom from alternative formulations of $Ru^{II}(EtOH)_2$ and $Ru^{IV}(OEt)_2$. These alternatives are difficult to distinguish crystallographically. A hydrogen-bonding scheme involving the solvent ethanol molecules as well as coordinated ethanol and ethoxide ligands suggests the formulation of this compound as Ru(III). Such a formulation is also consistent with the fact that complex **10** is paramagnetic with a solution magnetic moment (μ_{eff} = 1.6 μ_B) corresponding to one unpaired spin.[48]

The unit cell drawing for Ru(TPP)(OEt)(EtOH)·2EtOH in Figure 8[23] clearly shows the one-dimensional hydrogen-bonding chain directed along the *a* axis of the crystal. The intermolecular oxygen distances O(1)···O(2) = 2.591 (4) Å and O(2)···O(2′) = 2.641 (8) Å are in the range for hydrogen bonds of medium strength. The proposed placement of the hydrogen atoms for this system is presented in Figure 9. Since the ruthenium atom is constrained to lie on a crystallographic inversion center, there is disorder between the coordinated ethanol and ethoxide ligands. Such disorder, which probably is a manifestation of the lack of communication among the chains, is not shown in Figure 9.

Although the crystallographically imposed symmetry of Ru(TPP)(OEt)(EtOH) is only C_i, the structure very nearly possesses D_{4h} symmetry so that chemically equivalent bonds are approximately equal. These bond lengths and angles have been averaged in Table XII.

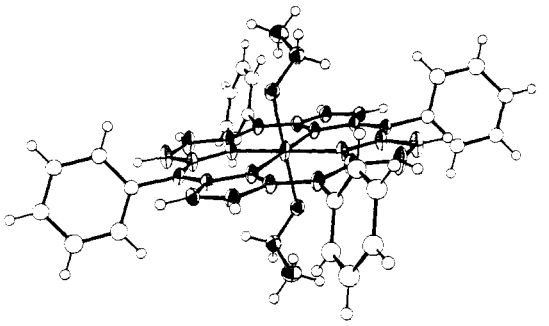

Figure 10. Drawing of Ru(TPP)(OEt)(EtOH), with non-hydrogen atoms drawn with 50% probability ellipsoids. Hydrogen atoms are drawn artificially small. The hydrogen atom on the coordinated ethanol group has been omitted.

Few structures of ruthenium porphyrin molecules are reported in the literature. The four reports are as follows: Ru(TPP)(CO)(py),[8a] Ru(TPP)(CO)(EtOH),[8b] which had originally been reported as $Ru(TPP)(CO)_2$,[49] $Ru(OEP)(py)_2$,[14b] and the Ru(IV) dimer $[Ru(OEP)(OH)]_2O$.[17] Table XIII contains averaged values of the structural parameters for these compounds and for compounds **10** and **2c** reported herein. In the averaging process D_{4h} symmetry has been assumed for the monomers and D_{4d} symmetry for the dimers. Differences between compound **10** and the Ru(II) and Ru(IV) porphyrins are few. Owing to the large standard deviations reported for both Ru(IV) dimer structures, it is difficult to observe any structural trends that result from the various oxidation states for ruthenium.

The geometry about the ruthenium atom in the Ru(III) porphyrin complex **10** may be described as a slightly distorted octahedron, as shown in Figure 10. The Ru(III)–N distance of 2.040 (6) Å in this compound is about the same as the previously reported Ru(II)–N bond lengths,[8a] but it is significantly shorter than the 2.104 (4)-Å length observed in $[Ru(NH_3)_6]^{3+}$.[50] The Ru–O(1) bond length of 2.019 (3) Å is slightly shorter than the sum of the ionic radii for Ru(III) and O^{2-} (2.05 Å),[51] and it is significantly shorter than the 2.21 (2)-Å value reported for Ru–O(Et) in Ru(TPP)(CO)(EtOH).[8b] The remaining bond lengths and angles in the macrocycle are typical for a porphyrin core.[22]

Table XIV[23] contains various least-squares planes through molecule **10**. Although the bond lengths and angles approximate to D_{4h} symmetry, the deviations of the atoms from a plane through the 24-atom porphyrin skeleton do not. However, these deviations are of the same order of magnitude as those found in Ru(TPP)(CO)(EtOH)[8b] and represent only small distortions from planarity. The dihedral angles between the mean plane of the porphyrin and the two phenyl groups are in the range 66–69° for **10**. The average C_m–C_p bond length of 1.508 Å can be interpreted to result from pure σ bonding between trigonally hybridized carbon atoms.[52] The CA(1)–O(1)–Ru–N(1) torsion angle of 28° places the projection of the CA(1) atom onto the porphyrin plane approximately halfway between the N and C_m atoms.

While the bond lengths and angles for the coordinated ethanol molecule seem normal, those for the solvent do not. This disordered ethanol has large thermal parameters and atypical bond lengths and angles with large errors. Although this model may not be completely satisfactory, it did permit the structure to reach convergence during refinement and appears to describe adequately the electron density in this region.

Our observations show that molecular oxygen oxidizes $Ru^{II}(TPP)(THF)_2$ (**5**) by 2 equiv in noncoordinating solvents to form the Ru(IV) oligomers, but in the presence of ethanol the oxidation halts at the Ru(III) state. The chemistry of ruthenium porphyrins

(47) Collman, J. P.; Brauman, J. I.; Doxsee, K. M. *Proc. Natl. Acad. Sci. U.S.A.* **1979**, *76*, 6035–6039.
(48) (a) Evans, D. F. *J. Chem. Soc.* **1959**, 2003–2005. (b) Live, D. H.; Chan, S. I. *Anal. Chem.* **1970**, *42*, 791–792.
(49) Cullen, D.; Meyer, E., Jr.; Srivastava, T. S.; Tsutsui, M. *J. Chem. Soc., Chem. Commun.* **1972**, 584–585.
(50) Stynes, H. C.; Ibers, J. A. *Inorg. Chem.* **1971**, *10*, 2304–2308.
(51) Huheey, J. E. "Inorganic Chemistry"; Harper and Row: New York, 1972; p 74.
(52) Radonovich, L. J.; Bloom, A.; Hoard, J. L. *J. Am. Chem. Soc.* **1972**, *94*, 2073–2078.

Table XII. Selected Distances (Å) and Angles (deg) in Ru(TPP)(OEt)(EtOH)·2EtOH (**10**)

Ru–N(1)	2.044 (3)	Ct···N[a]	2.040 (6)	C(2)–C(3)	1.351 (5)		
Ru–N(2)	2.036 (3)			C(7)–C(8)	1.348 (6)	C_b–C_b	1.350 (6)
Ru–C(1)	3.057 (4)			C(1)–C(10′)[c]	1.404 (5)		
Ru–C(4)	3.081 (4)	Ct···C_a	3.068 (12)	C(4)–C(5)	1.394 (5)	C_a–C_m	1.398 (5)
Ru–C(6)	3.074 (4)			C(6)–C(5)	1.396 (5)		
Ru–C(9)	3.058 (4)			C(9)–C(10)	1.397 (5)		
Ru–C(5)	3.456 (4)	Ct···C_m	3.444 (18)	C(5)–C(11)	1.510 (5)	C_m–C_p	1.508 (6)
Ru–C(10)	3.431 (4)			C(10)–C(17)	1.504 (6)		
Ru–O(1)	2.019 (3)			O(1)–CA(1)	1.413 (5)		
N(1)–C(1)	1.376 (5)			CA(1)–CB(1)	1.513 (6)		
N(1)–C(4)	1.373 (5)	N–C_a	1.377 (5)[b]	O(2)–CA(2)	1.323 (10)		
N(2)–C(6)	1.381 (5)			CA(2)–CB(2)	1.371 (11)		
N(2)–C(9)	1.378 (5)			CB(2)–CB(2′)	1.399 (14)		
C(1)–C(2)	1.439 (5)			O(2)–O(2′)	2.641 (8)		
C(4)–C(3)	1.433 (5)	C_a–C_b	1.437 (5)	O(1)–O(2)	2.591 (4)		
C(6)–C(7)	1.434 (5)						
C(9)–C(8)	1.440 (5)						
N(1)–Ru–N(2)	89.1 (1)			C(1)–C(2)–C(3)	107.3 (3)		
N(1)–Ru–N(2′)	90.9 (1)	N–Ru–N	90.0 (13)	C(4)–C(3)–C(2)	107.3 (3)	C_a–C_b–C_b	107.4 (4)
N(1)–Ru–O(1)	86.2 (1)			C(6)–C(7)–C(8)	107.8 (4)		
N(1′)–Ru–O(1)	93.8 (1)			C(9)–C(8)–C(7)	107.2 (4)		
N(2)–Ru–O(1)	89.4 (1)			N(1)–C(1)–C(10′)	125.9 (3)		
N(2′)–Ru–O(1)	90.6 (1)			N(1)–C(4)–C(5)	125.0 (4)	N–C_a–C_m	125.6 (4)
Ru–O(1)–CA(1)	124.5 (2)			N(2)–C(6)–C(5)	125.5 (4)		
O(1)–CA(1)–CB(1)	111.6 (3)			N(2)–C(9)–C(10)	125.6 (4)		
Ru–N(1)–C(1)	125.6 (3)			C(4)–C(5)–C(6)	125.4 (4)		
Ru–N(1)–C(4)	127.6 (3)	Ct···N–C_a	126.7 (9)	C(9)–C(10)–C(1′)	125.7 (4)	C_a–C_m–C_a	125.6 (4)
Ru–N(2)–C(6)	127.2 (3)			C(3)–C(4)–C(5)	125.4 (4)		
Ru–N(2)–C(9)	126.2 (3)			C(2)–C(1)–C(10′)	124.9 (4)	C_b–C_a–C_m	125.2 (4)
N(1)–C(1)–C(2)	109.2 (3)			C(7)–C(6)–C(5)	125.4 (4)		
N(1)–C(4)–C(3)	109.5 (3)	N–C_a–C_b	109.3 (3)	C(8)–C(9)–C(10)	125.1 (4)		
N(2)–C(6)–C(7)	109.1 (3)			C(4)–C(5)–C(11)	117.7 (4)		
N(2)–C(9)–C(8)	109.3 (3)			C(6)–C(5)–C(11)	116.9 (4)	C_a–C_m–C_p	117.2 (6)
C(1)–N(1)–C(4)	106.6 (3)	C_a–N–C_a	106.6 (3)	C(9)–C(10)–C(17)	117.8 (4)		
C(9)–N(2)–C(6)	106.6 (3)			C(1′)–C(10)–C(17)	116.5 (4)		
				O(2)–CA(2)–CB(2)	94.2 (7)		
				O(2)–CB(2)–CB(2′)	96.4 (8)		

[a] The nomenclature Ct, C_a, C_b, and C_m is defined by J. L. Hoard in ref 18a. The symbol C_p refers to the phenyl carbon bonded to the porphyrin ring. [b] Average values are weighted; the error is taken as the larger of the unweighted estimated standard deviation of a single observation and that estimated from the inverse least-squares matrix. [c] Primed atoms are related to corresponding unprimed atoms by the center of inversion.

Table XIII. Averaged Bond Lengths (Å) and Angles (deg) for Some Ruthenium Porphyrin Complexes

	Ru(TPP)(CO)(py)[a,b]	Ru(TPP)-(CO)-(EtOH)[a,c]	Ru(OEP)(py)$_2$[a,d]	Ru(TPP)-(OEt)-(EtOH)[e] (**10**)	[Ru(TPP)(*p*-$OC_6H_4CH_3$)]$_2$O[e] (**2c**)	[Ru(OEP)(OH)]$_2$O[a,f]
Ru–N	2.052 (9)[g]	2.049 (5)	2.047	2.040 (6)	2.050 (14)	2.067 (14)
N–C_a	1.370 (9)	1.374 (8)	1.367	1.377 (5)	1.375 (23)	1.372 (32)
C_a–C_m	1.395 (10)	1.393 (10)	1.40	1.398 (5)	1.391 (23)	1.405 (33)
C_a–C_b	1.446 (11)	1.437 (13)	1.45	1.437 (5)	1.436 (24)	1.456 (29)
C_b–C_b	1.333 (11)	1.327 (12)	1.32	1.350 (6)	1.352 (23)	1.315 (27)
C_a–N–C_a	107.8 (6)	107.4 (6)		106.6 (3)	108.0 (15)	107.3 (15)
N–C_a–C_b	108.3 (8)	108.3 (6)		109.3 (3)	108.3 (17)	108.4 (17)
N–C_a–C_m	126.4 (7)	125.6 (6)		125.6 (4)	126.3 (18)	125.5 (16)
C_a–C_b–C_b	107.8 (8)	108.0 (8)		107.4 (4)	107.6 (18)	107.8 (17)
C_a–C_m–C_a	125.0 (7)	126.1 (6)		125.6 (4)	124.9 (18)	126.2 (17)

[a] Data collected at room temperature. [b] Reference 8a. [c] Reference 8b. [d] Reference 14b. Crystallographic details for this compound are sketchy. No errors or bond angles are reported. The averaged bond lengths reported here are for one of the two independent centrosymmetric molecules. [e] This work. [f] Reference 17. [g] Error in mean value is the larger of the unweighted estimated standard deviation of a single observation and the error estimated from the least-squares inverse matrix. Averaging has been done assuming D_{4h} symmetry for the monomers and D_{4d} symmetry for the dimers.

with oxygen is summarized in Scheme III. Three points of significance arise from this chemistry: (i) Few examples of ruthenium(III) porphyrin complexes are known. The Ru(III) and Ru(IV) species described herein are the first products of the reactions of ruthenium porphyrins with molecular oxygen to be structurally characterized. (ii) Our results, and those of others,[6] indicate that the interaction of oxygen with ruthenium porphyrins is highly solvent dependent. (iii) The conversion of Ru(II) and Ru(III) porphyrins to stable Ru(IV) species through the use of dioxygen as the oxidant has no precedent in iron porphyrin chemistry.

In the light of our results a discussion of the few studies reported in the literature on the interactions of dioxygen with ruthenium and osmium porphyrins is relevant here. Two examples of ruthenium complexes containing other nitrogen donor ligands are also of interest. The first Ru(III) porphyrin complex to be reported was $[Ru(TPP)(CN)_2]^+$, produced by air oxidation of Ru(TPP)(CO) in the presence of cyanide ion.[7] Barley et al. have prepared a Ru(III) cation radical complex[42] and have invoked the presence of Ru(III) autoxidation products in studies on the oxygenation of Ru(II) porphyrins.[6] Farrel et al. have reported that Ru(OEP)$(MeCN)_2$ in dimethylacetamide, dimethylformamide, or pyrrole absorbs 1.0 mol of O_2 per Ru to yield an oxygenated species.[6a] This product has been characterized only by electronic spectroscopy. The reaction can be reversed by pumping on the oxygenated solution or by purging it with CO, although in toluene solution slow, irreversible oxidation of the Ru(II) precursor was observed. Reversible oxygenation of Ru(II) por-

Scheme III

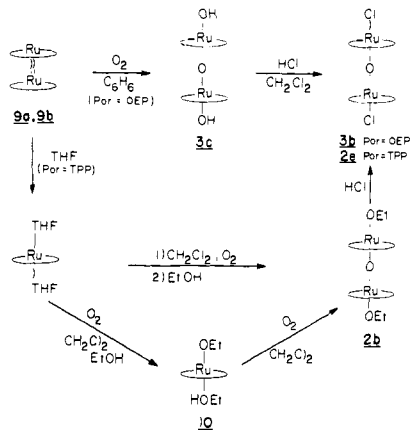

phyrins in condensed monolayer systems has also been reported.[4b]

The Os(II) complex $Os(OEP)(py)_2$ is air oxidized to $[Os^{III}(OEP)(py)_2]^+$ with corresponding formation of $^1/_2H_2O_2$. The mechanism proposed involves outer-sphere electron transfer as the strongly coordinating pyridine ligands preclude the existence of an open coordination site.[53]

In aqueous solution $[Ru^{III}(NH_3)_5(py)]^{3+}$ disproportionates above a pH of 8 to Ru(II) and Ru(IV) species.[54] The Ru(II) product is oxidized by oxygen to Ru(III), and thus the process can be driven to the Ru(IV) product. The driving force for the disproportionation is the acidity of the ammine protons in the Ru(IV) species. We can discount such a mechanism in our system as the Ru(IV) oligomers are formed in the less basic, aprotic medium.

Chemistry very similar to the formation of **10** from **5** has been observed in the work of Durham et al. with *trans*-$[Ru^{II}(bpy)_2(OH_2)_2]^{2+}$.[55] In an acidic aqueous medium this complex is oxidized by air to *trans*-$[Ru^{III}(bpy)_2(OH_2)(OH)]^{2+}$. An X-ray structural characterization of the Ru(III) product shows that it has crystallographically imposed C_2 symmetry with equivalent axial ligands. The structure consists of infinite chains of *trans*-Ru(III) cations linked by symmetrical hydrogen bonds. The Ru–O bond length of 2.007 (3) Å is the same as that of 2.019 (3) Å measured for **10**, and the hydrogen-bonding schemes in the two structures are similar. The pK_a values for $[Ru^{III}(bpy)_2(py)(OH_2)]^{3+}$ and $[Ru^{II}(bpy)_2(py)(OH_2)]^{2+}$ are 0.85 and 10.8, respectively.[55] It is not surprising then that both $[Ru^{III}(bpy)_2(OH_2)(OH)]^{2+}$ and **10** have lost this very acidic proton.

The presence of a Ru(II) dioxygen complex can be invoked but has not been confirmed in any of these systems, including the present one. We have isolated and characterized stable Ru(III) and Ru(IV) species formed by the interaction of dioxygen with Ru(II) precursors and have demonstrated that the oxidation processes are solvent dependent. These observations may be helpful in elucidating the chemistry of any transient oxygenated species.

Autoxidation of Fe(II) dioxygen complexes invariably leads to the formation of Fe(III) μ-oxo dinuclear species. In contrast, in ruthenium porphyrin chemistry it appears that the corresponding μ-oxo oligomers, formed in the presence of oxygen or other oxidizing agents, are in the +IV oxidation state. This result may reflect the greater stability of the second- and third-row members of a triad in the higher oxidation states. This observed stability of ruthenium in higher oxidation states may be of value in attempts to model high oxidation state intermediates in systems such as cytochrome P450.

Acknowledgment. This work was supported by the National Institutes of Health, Grant GM 17880 (to J.P.C.) and Grant HL 13157 (to J.A.I.), and the National Science Foundation, Grant CHE78-09443 (to J.P.C.). Mass spectral analyses were carried out at the Middle Atlantic Mass Spectrometry Laboratory (Johns Hopkins University), a National Science Foundation Shared Instrumentation Facility. NMR spectra were recorded on instruments supported by the following grants: 360 MHz, NSF GP23633 and NIH RR00711 (Stanford Magnetic Resonance Laboratory); 100 MHz, NSF GP28142 and CHE77-08810 (Stanford University).

Registry No. **1a**, 41654-56-2; **1b**, 90554-87-3; **1c**, 89530-39-2; **2a**, 90554-88-4; **2b**, 90554-89-5; **2c**, 80004-25-7; **2d**, 90554-90-8; **2e**, 90554-91-9; **2f**, 90554-92-0; **2g**, 90554-93-1; **2h**, 90554-94-2; **3a**, 90554-95-3; **3b**, 80004-23-5; **3c**, 77089-60-2; **4a**, 90554-96-4; **4b**, 90554-97-5; **4c**, 90554-98-6; **5**, 90584-08-0; **6a**, 34690-40-9; **6b**, 90554-99-7; **8c**, 90555-00-3; **9a**, 80004-21-3; **10**, 90584-10-4; $RuCl_3$, 10049-08-8; dodecacarbonyltriruthenium(0), 15243-33-1.

Supplementary Material Available: For compound **2c** Table II, positional and thermal parameters of the non-group atoms, Table III, parameters for the rigid group atoms, Table IV, a listing of structure amplitudes, Table XI, least-squares planes, and Figure 5, stereodrawing of the unit cell; for compound **10**, Table V, positional and thermal parameters of the non-group atoms, Table VI, parameters for the rigid-group atoms, Table VII, root-mean-square amplitudes of vibration, Table VIII, structure amplitudes, Table XIV, least-squares planes, and Figure 8, stereodrawing of the unit cell (56 pages). Ordering information is given on any current masthead page.

(53) Billecke, J.; Kokishe, W.; Buchler, J. W. *J. Am. Chem. Soc.* **1980**, *102*, 3622–3624.
(54) Rudd, P. DeF.; Taube, H. *Inorg. Chem.* **1971**, *10*, 1543–1544.
(55) Durham, B.; Wilson, S. R.; Hodgson, D. J.; Meyer, T. J. *J. Am. Chem. Soc.* **1980**, *102*, 600–607.